VYSOKÉ UČENÍ TECHNICKÉ V BRNĚ

BRNO UNIVERSITY OF TECHNOLOGY

FAKULTA STAVEBNÍ

FACULTY OF CIVIL ENGINEERING

ÚSTAV TECHNICKÝCH ZAŘÍZENÍ BUDOV

INSTITUTE OF BUILDING SERVICES

ANALYSIS OF BOUNDARY CONDITIONS OF GROUND HEAT EXCHANGERS

ANALYSIS OF BOUNDARY CONDITIONS OF GROUND HEAT EXCHANGERS

DIPLOMOVÁ PRÁCE

DIPLOMA THESIS

AUTOR PRÁCE / AUTHOR: Bc. Skarleta Floreková

VEDOUCÍ PRÁCE / SUPERVISOR: prof. Ing. JIŘÍ HIRŠ, CSc.

BRNO 2021

VYSOKÉ UČENÍ TECHNICKÉ V BRNĚ
FAKULTA STAVEBNÍ

Studijní program	N3607 Stavební inženýrství
Typ studijního programu	Navazující magisterský studijní program s prezenční formou studia
Studijní obor	3608T001 Pozemní stavby
Pracoviště	Ústav technických zařízení budov

ZADÁNÍ DIPLOMOVÉ PRÁCE

Student	Bc. Skarleta Floreková
Název	Analysis of boundary conditions of ground heat exchangers
Vedoucí práce	prof. Ing. Jiří Hirš, CSc.
Datum zadání	31. 3. 2020
Datum odevzdání	15. 1. 2021

V Brně dne 31. 3. 2020

prof. Ing. Jiří Hirš, CSc.
Vedoucí ústavu

prof. Ing. Miroslav Bajer, CSc.
Děkan Fakulty stavební VUT

PODKLADY A LITERATURA

Applicable laws, ordinances, regulations and standards related to the solving theme of diploma thesis. Domestic, European and world literature, proceedings of scientific conferences and professional events in the field of HVAC. Sources on the Internet. Data from solved building and devices.

Detailed information and further clarification of diploma thesis provides supervisor during consultation.

ZÁSADY PRO VYPRACOVÁNÍ

A. Theoretical part - a literature review of a given topic, range 10 to 15 pages

B. Calculation part

B1. Diagnostic of external and internal boundary conditions of ground heat distribution in spa

B2. Analysis of boundary conditions of the ground heat exchangers

• proposals for measures to reduce energy consumption

• evaluation of the proposed measures

C. Project

• application of calculation methods to the part of ground heat exchangers in the spa

• elaboration of solutions to increase of effectivity heat transfer

• description of created schemes and solutions

D. conclusion, list of sources, the list of abbreviations and symbols, list of annexes, attachments - drawings, diagrams

STRUKTURA DIPLOMOVÉ PRÁCE

VŠKP vypracujte a rozčleňte podle dále uvedené struktury:

1. Textová část závěrečné práce zpracovaná podle platné Směrnice VUT "Úprava, odevzdávání a zveřejňování závěrečných prací" a platné Směrnice děkana "Úprava, odevzdávání a zveřejňování závěrečných prací na FAST VUT" (povinná součást závěrečné práce).

2. Přílohy textové části závěrečné práce zpracované podle platné Směrnice VUT "Úprava, odevzdávání, a zveřejňování závěrečných prací" a platné Směrnice děkana "Úprava, odevzdávání a zveřejňování závěrečných prací na FAST VUT" (nepovinná součást závěrečné práce v případě, že přílohy nejsou součástí textové části závěrečné práce, ale textovou část doplňují).

prof. Ing. Jiří Hirš, CSc.

Vedoucí diplomové práce

ABSTRACT

Master thesis ,,Analysis of boundary conditions of ground heat exchangers,, is primarily focused on analysis of boundary conditions and major factors affecting a reliable design and heat transfer of horizontal ground heat exchanger in the area of geothermal activities at Spa Island in Piešťany. Assessments of its possible environmental impacts such as an origin of subsoil thermal alterations due to the heat extraction including a soil freezing around the pipelines and potentially contamination of groundwater are discussed too. As a part of this final thesis, three numerical analyses were processed using finite element method software COMSOL Multiphysics 5.6., which may occur in this specific area.

The first numerical analysis is subjected on study of dynamic processes of horizontal ground heat exchanger and saturated subsoil under the constant boundary temperature condition of the ground. Dynamic process of ground heat exchanger and saturated subsoil under the inconstant temperature boundary condition is examined in the second numerical analysis. The last analysis is carried out to assessments the horizontal ground heat exchanger operation with possibility of groundwater flow in the same strata. Thanks to these numerical studies and dynamic thermal models results, each study case contains soil temperature distributions, outlet temperatures from the exchanger and its own partial conclusion.

KEYWORDS

ground heat exchanger, renewable source energy, boundary condition, dynamic process, heat transfer, porous medium, groundwater flow, saturated soil, thermal conductivity

ABSTRAKT

Diplomová práca,, ,,Analysis of boundary conditions of ground heat exchangers,, je primárne zameraná na analýzu okrajových podmienok a hlavných faktorov vplývajúcich na spoľahlivý návrh a prestup tepla plošného zemného výmenníka v oblasti geotermálnych aktivít na kúpeľnom ostrove v Piešťanoch. Posúdenie možných vplyvov na životné prostredie, ako je napríklad vznik tepelných zmien v dôsledku extrakcie tepla vrátane zamŕzania pôdy v okolí potrubia a potenciálneho znečistenia podzemných vôd je taktiež rozoberané. Súčasťou tejto záverečnej práce boli spracované tri numerické analýzy metódou konečných prvkov pomocou softvéru COMSOL Multiphysics 5.6., ktoré sa môžu vyskytnúť v tejto konkrétnej oblasti.

Prvá numerická analýza je podrobená štúdii dynamických procesov plošného zemného výmenníka tepla a zeminy nasýtenou vodou pri konštantnej teplotnej okrajovej podmienke pôdy. Dynamický proces zemného výmenníka tepla a nasýteného podložia pri nestálej teplotnej okrajovej podmienke je skúmaný v druhej numerickej analýze. Posledná analýza je vyhotovená na posúdenie prevádzky plošného zemného výmenníka tepla s možnosťou prúdenia podzemnej vody v rovnakej vrstve. Vďaka týmto numerickým štúdiám a výsledkom dynamických tepelných modelov, každá prípadová štúdia obsahuje rozloženie teplôt v zemine, výstupné teploty z výmenníka a vlastný čiastočný záver.

KĽÚČOVÉ SLOVÁ

zemný výmenník tepla, obnoviteľný zdroj energie, okrajová podmienka, dynamický proces, prestup tepla, pórovité médium , prúdenie podzemnej vody, vodou nasýtená zemina, tepelná vodivosť

BIBLIOGRAFICKÁ CITACE

Bc. Skarleta Floreková *Analysis of boundary conditions of ground heat exchangers.* Brno, 2021. 83 s., 9 s. příl. Diplomová práce. Vysoké učení technické v Brně, Fakulta stavební, Ústav technických zařízení budov. Vedoucí práce prof. Ing. Jiří Hirš, CSc.

PROHLÁŠENÍ O SHODĚ LISTINNÉ A ELEKTRONICKÉ FORMY ZÁVĚREČNÉ PRÁCE

Prohlašuji, že elektronická forma odevzdané diplomové práce s názvem *Analysis of boundary conditions of ground heat exchangers* je shodná s odevzdanou listinnou formou.

V Brně dne 15. 1. 2021

Bc. Skarleta Floreková
autor práce

PROHLÁŠENÍ O PŮVODNOSTI ZÁVĚREČNÉ PRÁCE

Prohlašuji, že jsem diplomovou práci s názvem *Analysis of boundary conditions of ground heat exchangers* zpracovala samostatně a že jsem uvedla všechny použité informační zdroje.

V Brně dne 15. 1. 2021

Bc. Skarleta Floreková
autor práce

Acknowledgments:

I would like to express my deepest gratitude to my supervisor, prof. Ing. Jiří Hirš, CSc. for his valuable comments, inspiring guidance and assistance in writing of master thesis Analysis of boundary conditions of ground heat exchanger. Secondly I would like to express my gratitude to Ing. Martin Kožíšek from HUMUSOFT company for a opportunity to use software COMSOL Multiphysics within this final thesis and for his helpful guidance through modelling.

In Brno 15. 01. 2021

....

Signature of author

Bc. Skarleta Floreková

CONTENT

1. INTRODUCTION

Currently, one of a world´s global problem is use of fossil fuels including oil, coal and natural gas that lead to environmental pollution around us. Using of renewable energy sources is a perspective way to improve environmental ecology and energy efficiency. Ground source heat pumps use a low energy stored in the subsoil and it is used for heating and cooling of buildings, as it is a highly efficient, reliable and sustainable technology that significantly contributes to the reduction of greenhouse gas emission, according to the targets set by the European Union.

An important element of low-potential energy collection system is ground heat exchanger. An energy efficiency and performance of heat exchangers strongly depends on site-specific properties of the ground. A several factors have to be considered to choose the right ground system for a particular installation in an early stage of any project. These factors include a geological characteristic of interest location and hydrology. Neglecting the above-mentioned aspects can result in negative environmental impacts such as a monumental thermal alterations origin of subsoil due to the heat extraction including a soil freezing around the pipelines and ground contamination and potentially contamination of groundwater too. Assessing the subsurface thermal impact of horizontal ground heat exchanger is therefore essential for their design. An evaluation of these adverse effects can be solved either analytically or numerically. By numerical methods, the reliable estimations are achieved.

Master thesis ,,Analysis of boundary conditions of ground heat exchangers" aim on analysis of boundary conditions affecting the reliable design of horizontal ground heat exchanger and heat transfer in area of geothermal activities at Spa Island in Piešťany. Assessments of its environmental impacts are discussed too. The analysis carried out in this final thesis is processed numerically using commercial software COMSOL Multiphysics 5.6., which allowed determining long-term temperature changes at various depth of subsoil related to the operation of the ground heat exchanger. This software works within the finite element method framework.

Modelling of heat transfer processes creating thermal regime of a multi-component system is an extremely demanding task and to understand it one must be subdivide it into its constituent elements and facets. There are more than a few circumstances influencing a heat transfer efficiency and heat rate of heat exchanger which are included in. Three possible cases that may occur in this study were investigated. The first numerical analysis is subjected to dynamic process of saturated subsoil under the constant boundary temperature condition during 1 year-round running of ground heat exchanger. The second numerical analysis is subjected to dynamic process of saturated subsoil under the inconstant boundary temperature condition during 1 year-round running of ground heat exchanger. The last analysis was carried out to assessment the horizontal ground heat exchanger operation with possibility of groundwater flow.

2. THEORETICAL PART

Theoretical part is aimed on a literature review of given topic concerning law definitions, technological equipment characterization and literature review of thermodynamics.

2.1. EUROPEAN ENERGY UNION

European Union´s energy policies aim to ensure that European citizens can access secure, affordable and sustainable energy supplies. The EU is working in a number of areas to make this happen. The energy union strategy, was adopted on 25 February 2015. [12]

According to the Energy Union (2015), the five main aims of the EU's energy policy are to: [12]

- ensure the functioning of the internal energy market and the inter-connection of energy networks (Chart 2.1.);
- ensure security of energy supply in the Union;
- promote energy efficiency and energy saving;
- promote the development of new and renewable forms of energy to better align and integrate climate change goals into the new market design;
- promote research, innovation and competitiveness.

As a part of its long-term energy strategy, the EU has set targets for 2020 and 2030. These cover emissions reduction, improved energy efficiency, and an increased share of renewable in the European Union´s energy mix. It has also created an Energy Roadmap for 2050, in order to achieve its goal of reducing greenhouse gas emissions by 80 – 95 %, when compared to 1990 level, by 2050. [12]

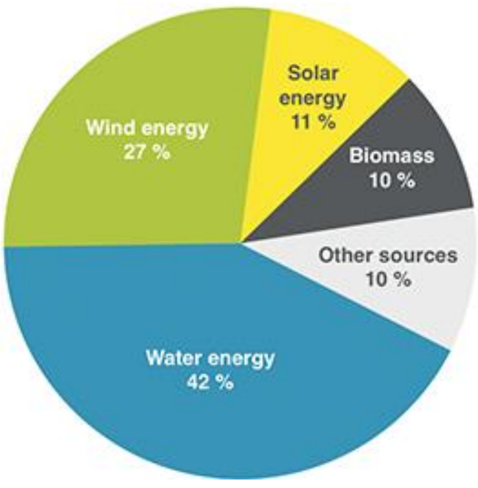

Chart 2.1. – The share of individual renewable energy sources within countries in the European Union

2.1.1. Targets 2020

By 2020, the EU aims to reduce its greenhouse gas emissions by at least 20%, increase the share of renewable energy to at least 20% of consumption, and achieve energy savings of 20% or more. All EU countries must also achieve a 10% share of renewable energy in their transport sector (Picture 2.1.). [12]

In order to meet the targets, the 2020 Energy Strategy sets out an five priorities: [12]

- making Europe more energy efficient by accelerating investment into efficient buildings, products, and transport. This includes measures such as energy labelling schemes, renovation of public buildings, and ecodesign requirements for energy intensive products;
- building a pan-European energy market by constructing the necessary transmission lines, pipelines, LNG terminals, and other infrastructure;
- protecting consumer rights and achieving high safety standards in the energy sector;
- implementing the *Strategic Energy Technology Plan* – the EU's strategy to accelerate the development and deployment of low carbon technologies such as solar power, smart grids, and carbon capture and storage;
- pursuing good relations with the EU's external suppliers of energy and energy transit countries. Through the Energy Community, the EU also works to integrate neighbouring countries into its internal energy market.

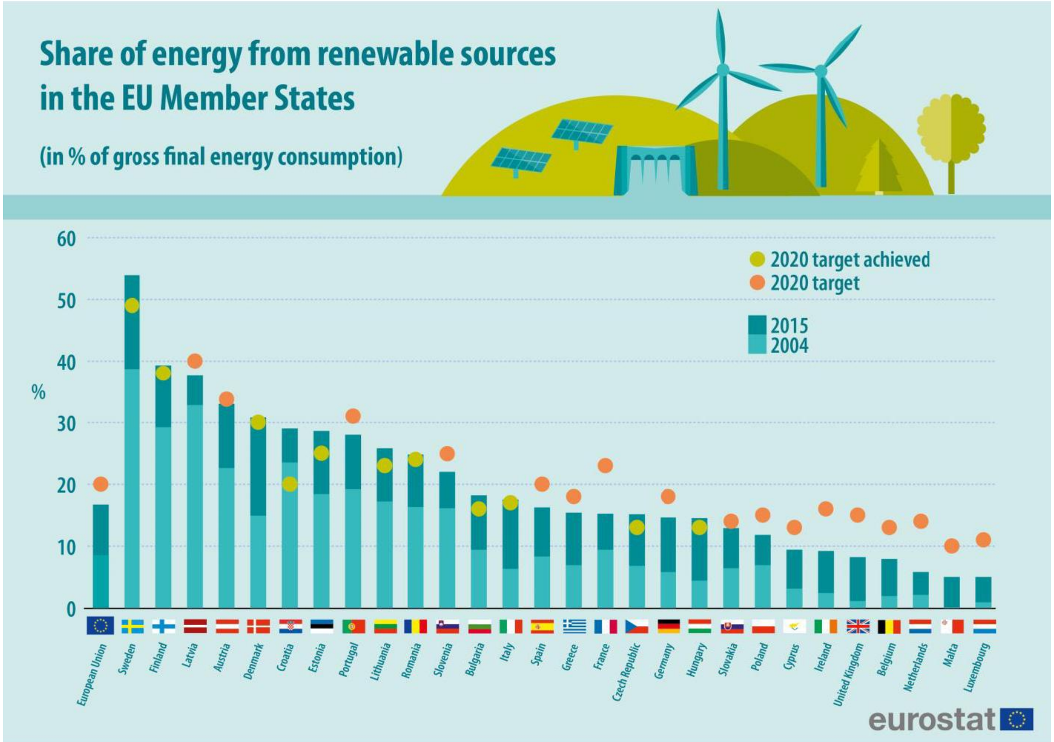

Picture 2.1. – The share of energy from renewable sources, 2004 and 2015 [12]

2.1.2. Targets 2050

The EU is committed to reducing greenhouse gas emissions to 80-95% below 1990 levels by 2050 in the context of necessary reductions by developed countries as a group 1, that it state in Picture 2.2. The Commission analysed the implications of this in its “Roadmap for moving to a competitive low-carbon economy in 2050”. The ”Roadmap to a Single European Transport Area” focussed on solutions for the transport sector and on creating a Single European Transport Area. In this Energy Roadmap 2050 the Commission explores the challenges posed by delivering the EU's decarbonisation objective while at the same time ensuring security of energy supply and competitiveness. It responds to a request from the European Council. [12]

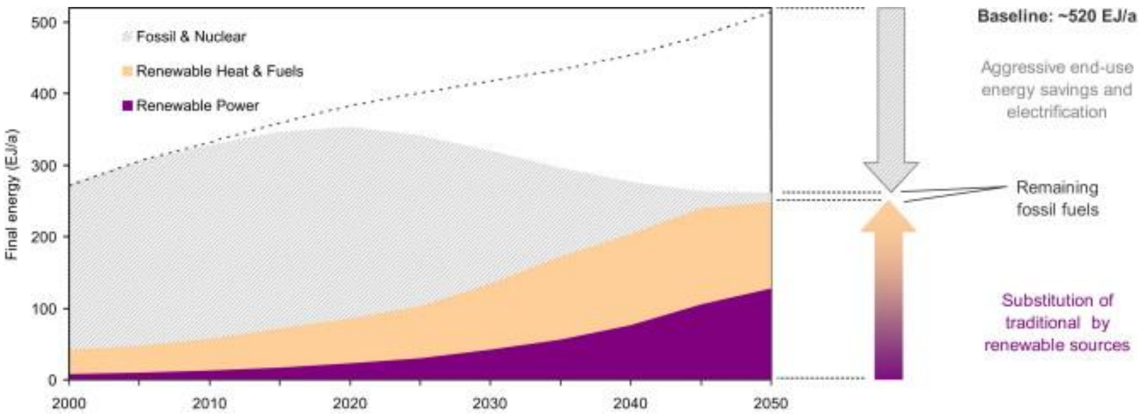

Picture 2.2. – 95 % renewable energy world by 2050 [1]

Even under this ambitious demand scenario, we’re still going to need about 260 EJ worth of final energy annually to power the planet. Where will it come from, and what do the report’s authors count as “sustainable” energy sources, are shown below in the Picture 2.3..

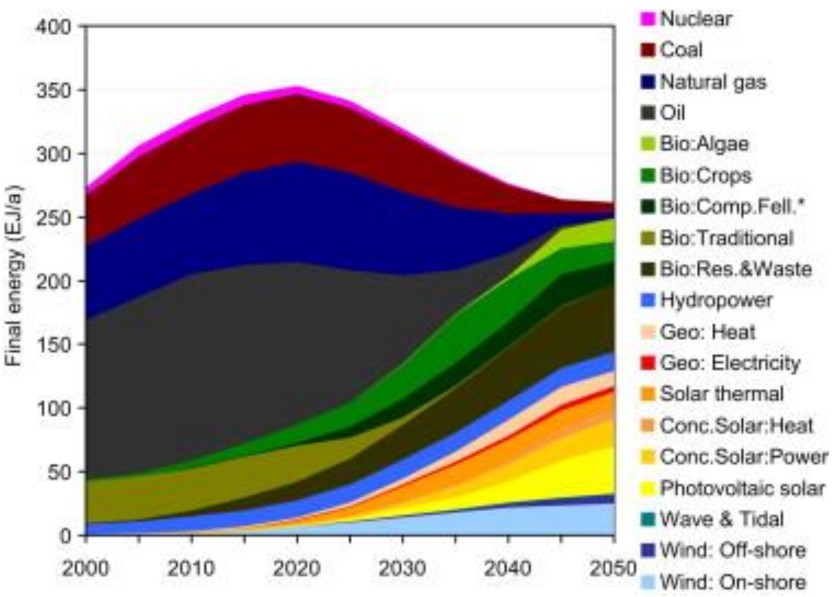

Picture 2.3. – Sustainable energy sources to power a our planet [1]

2.2. LEGISLATION OF RENEWABLE ENERGY SOURCES IN SLOVAKIA

The target which Slovakia is obligated to reach by 2020 is to produce 14 % of energy from renewable sources (currently about 8,7 %). The basic legal framework governed by the Act on Promotion of Renewable Energy and High-Efficiency Cogeneration No. 309/2009 Coll.. This is called feed in tariff law providing for certain support scheme. As of May 1 2010, with respect to requirements for the building of facilities producing energy, an amendment came into effect, which requires that the compliance of the investment certificate with the long-term energy policy is issued also for facilities producing electricity from solar sources with a capacity of 100 kW and more. [23]

According to the RES law, the following energy sources are eligible for support: hydro, solar, wind, geothermal, biomass, biogas and biomethane (Chart 2.2.).

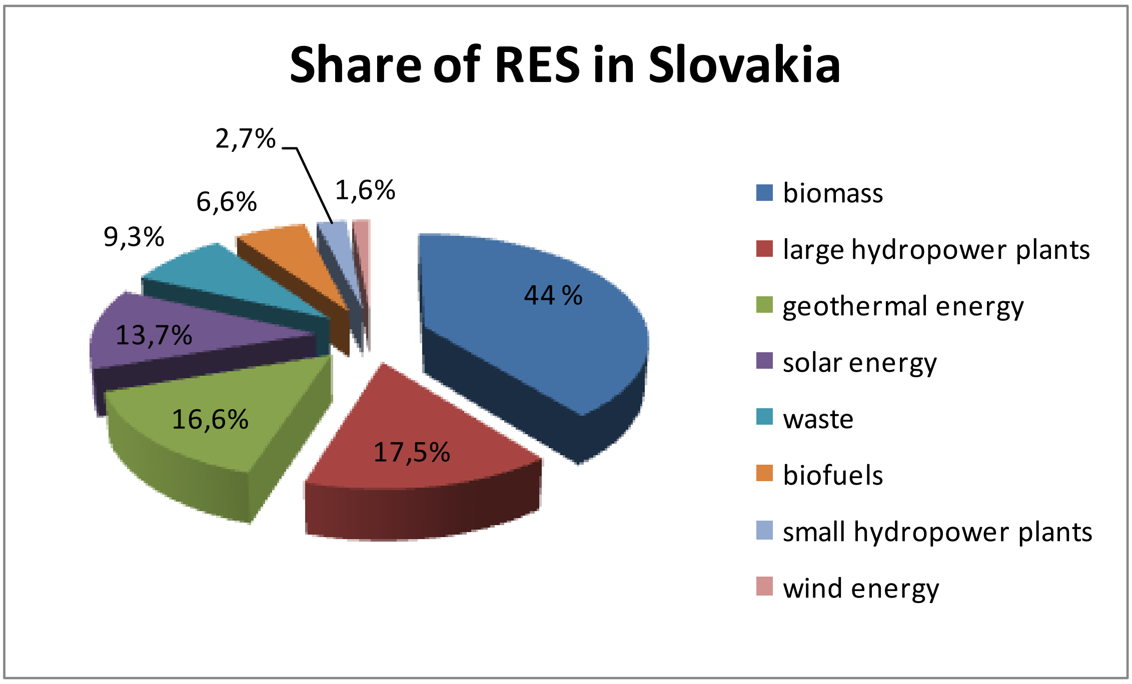

Chart 2.2. – The share renewable energy sources in Slovakia

2.3. GROUND SOURCE ENERGY

Ground source energy (Picture 2.4.) is a cost effective and low carbon solution for managing the energy requirement of any building, delivering both heating and cooling needs. Heat can be extracted from the ground via fluid circulating through an array of pipes in the ground to provide heating to buildings in winter. The ground acts as a "heat source". The ground can also be used as a "heat sink" for heat extracted from a building in summer in order to provide cooling. [19]

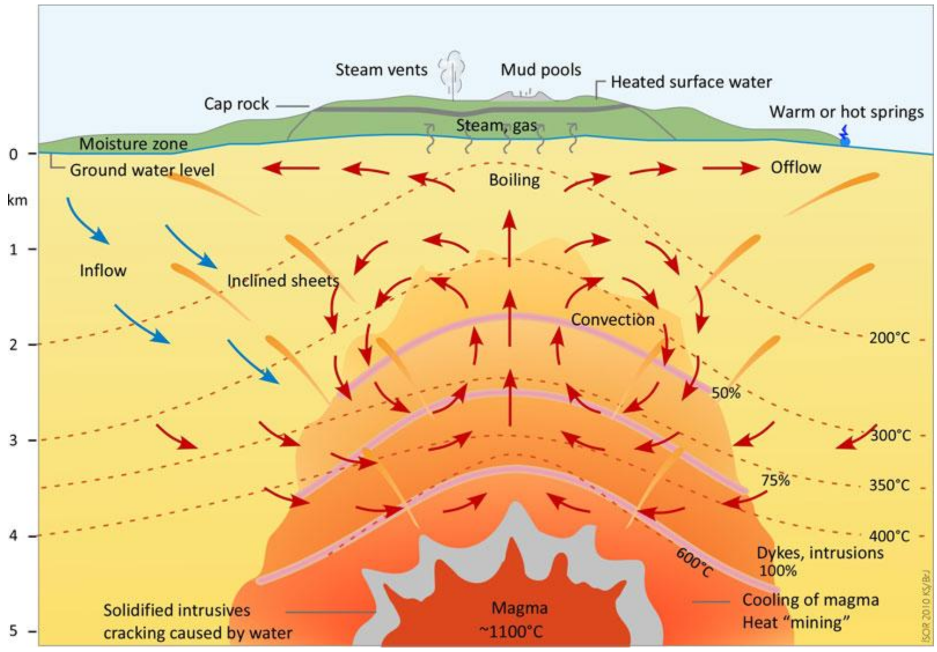

Picture 2.4. – Ground energy [20]

2.4. THERMODYNAMICS

Thermodynamics is a branch of physics which deals with the energy and work of a system. It was born in the 19th century as scientists were first discovering how to build and operate steam engines. Thermodynamics deals only with the large scale response of a system which we can observe and measure in experiments. [26]

There are three principal laws of thermodynamics: [26]

1. *Zeroth law* – if two thermodynamic systems are each in thermal equilibrium with a third one, then they are in thermal equilibrium with each other. Accordingly, thermal equilibrium between systems is a transitive relation.

2. *First law of thermodynamics* – energy conservation, the total energy of an isolated system is constant; energy can be transformed from one form to another

3. *Second law of thermodynamics* – the total entropy of an isolated system can never decrease over time. The total entropy of a system and its surroundings can remain constant in ideal cases where the system is in thermodynamic equilibrium, or is undergoing a (fictive) reversible process.

2.4.1. Heat transfer

Heat transfer is the process of transfer of heat from high temperature reservoir to low temperature reservoir. In terms of the thermodynamic system, heat transfer is the movement of heat across the boundary of the system due to temperature difference between the system and the surroundings. The difference in temperature is considered to be ‘potential’ that causes the flow of heat and the heat itself is called as flux. There are three types of heat transfer as a conduction, convection and radiation, that are shown in the Picture 2.5.. [6]

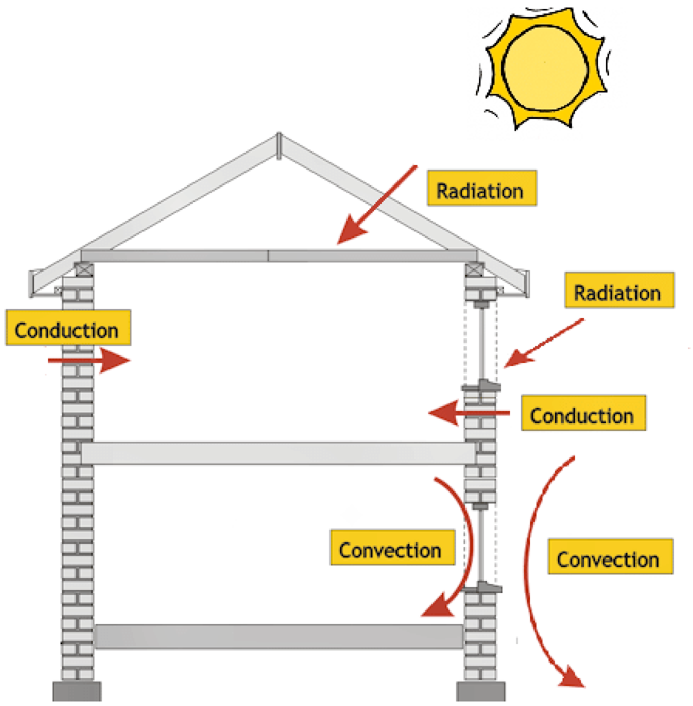

Picture 2.5. – Three types of heat transfer [29]

2.4.1.1. Conduction

The heat transfer between two solid bodies is called as conduction (Picture 2.6.). It depends on the difference in temperature of the hot and cold body. [6]

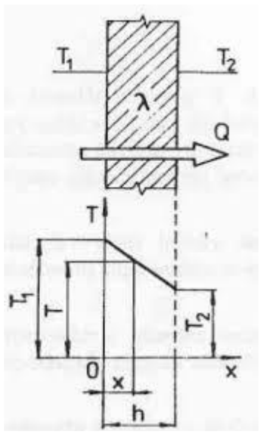

Picture 2.6. – Heat conduction by flat wall [7]

2.4.1.2. Convection

Heat transfer between the solid surface and the liquid as called as convection. This process is illustrated in the Picture 2.7. Convection can arise spontaneously (or naturally, freely) through the creation of convection cells or can be forced by propelling the fluid across the object or by the object through the fluid. [6]

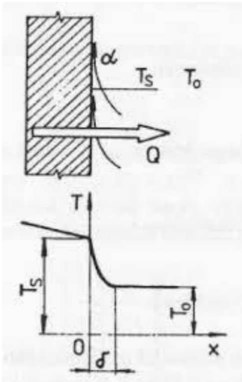

Picture 2.7. – Heat transfer by convection [7]

2.4.1.3. Radiation

When two bodies are at the different temperatures and separated by the distance, the heat transfer between them is called as radiation heat transfer. The radiation heat transfer occurs due to the electromagnetic waves that exist in the atmosphere. One of the most important examples of radiation heat transfer is the heat of sun coming on the earth. [6]

2.5. THE HEAT OF THE GROUND TRANSMITTED BY GROUNDWATER

Difference of heat transfer by conduction and convection are generally known. Therefore, special attention must be paid to convection heat transfer in the earth´s crust by water medium. The importance of water for heat transfer in the deeper layers of the Earth, in the surface layer of the continental crust, generally in hydrosphere or in lithosphere is great, especially with respect and understanding of use this heat. [30]

Heat transfer by water is heat movement by convection. The movement is very fast and can be implemented even over long distance. Hot water in the ground could be of dual origin: [30]

Meteoric water is water coming from atmospheric precipitation. By methods of isotope geochemistry has been proven, that most groundwater is solely of meteoric origin. By gravity descends infiltrated precipitation water through the cracks and in pores of rocks into the depth. Several kilometres under surface the groundwater are heated up to 200 °C or higher. This fact is illustrated in the Picture 2.8. [30]

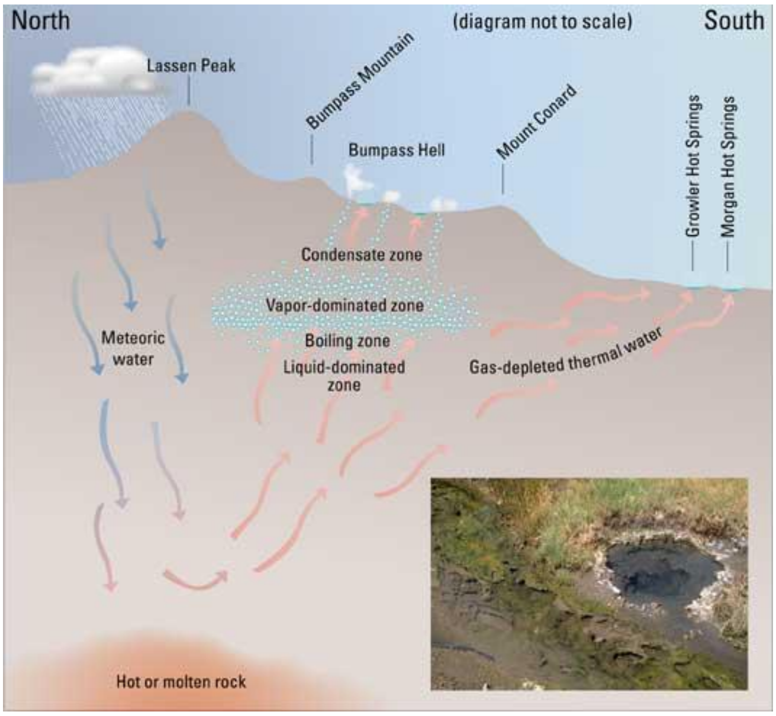

Picture 2.8. – Origin of hot meteoric water [41]

Juvenile water is ,, new" water, whose sources are metamorphic and geochemical processes of rocks in deeper layers of Earth (Picture 2.9.). During this processes the water is released from the rocks and as hot overheated water or steam escapes to the surface of the Earth with gases. [30]

Picture 2.9. – Juvenile water (hot springs) in Umi jikogu – Japan [46]

2.6. HEAT PUMP

A heat pump is an electrical device that extracts heat from one place and transfers it to another one. [18]

It consist of:

- evaporator;
- refrigerant;
- compressor;
- condenser unit;
- expansion valve;
- electric power.

The evaporator recovers heat from the environment (water, air, soil). In the evaporator, a refrigerant passes from liquid to gaseous state and then travels to the compressor. There, the vapours are compressed to increase pressure and temperature. Whole process and principle of heat pump works is illustrated bellow in the Picture 2.10. Hot vapours are liquefied in the condenser unit, emitting the condensation heat to the heating medium**.** Then the refrigerant passes through an expansion valve where its pressure is again lowered, and continues back to the evaporator where the process is repeated. Raising its temperature requires some energy. Hence, electric power is required for heat pump operation to power the compressor. [18]

There are three types of heat pumps:

- air/water;
- water/water;
- ground/water.

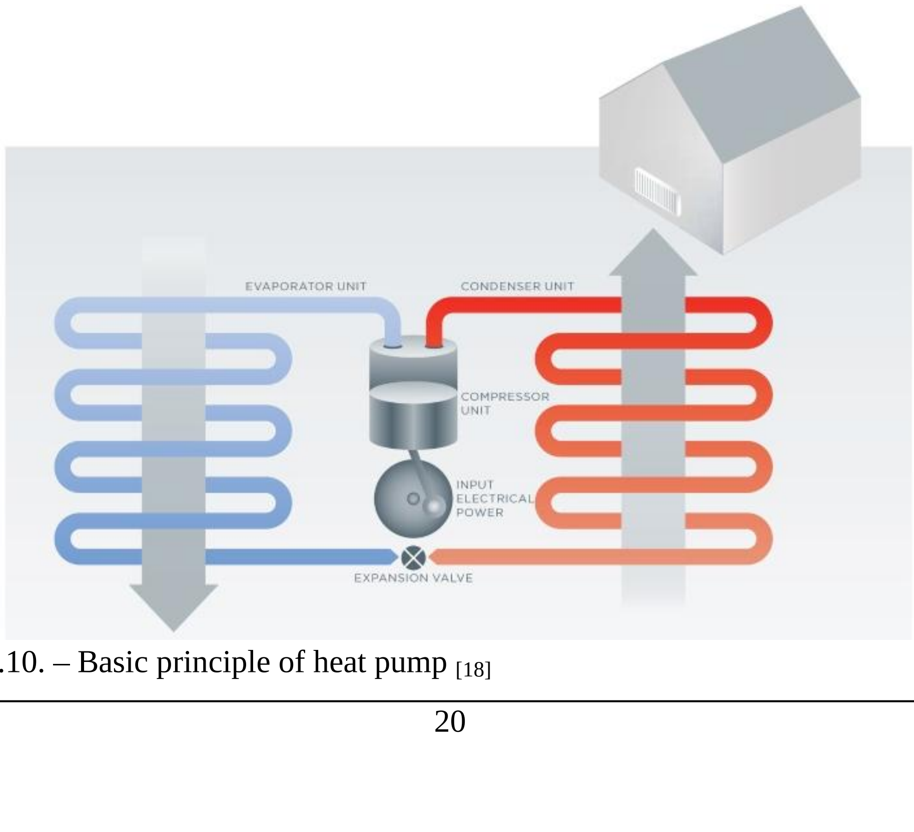

Picture 2.10. – Basic principle of heat pump [18]

2.6.1. Heat pump air/water

Air source heat pumps absorb heat from the outside air. This heat can then be used to the heat radiators, floor radiant heating systems, or warm air convectors and hot water, as shown below. Heat from the air is absorbed at low temperature into a fluid. This fluid then passes through a compressor where its temperature is increased, and transfers its higher temperature heat to the heating and hot water circuits of the house.[3]

An air-to-water system (Picture 2.11.) distributes heat via wet central heating system. Heat pumps work much more efficiently at a lower temperature than a standard boiler system would. [3]

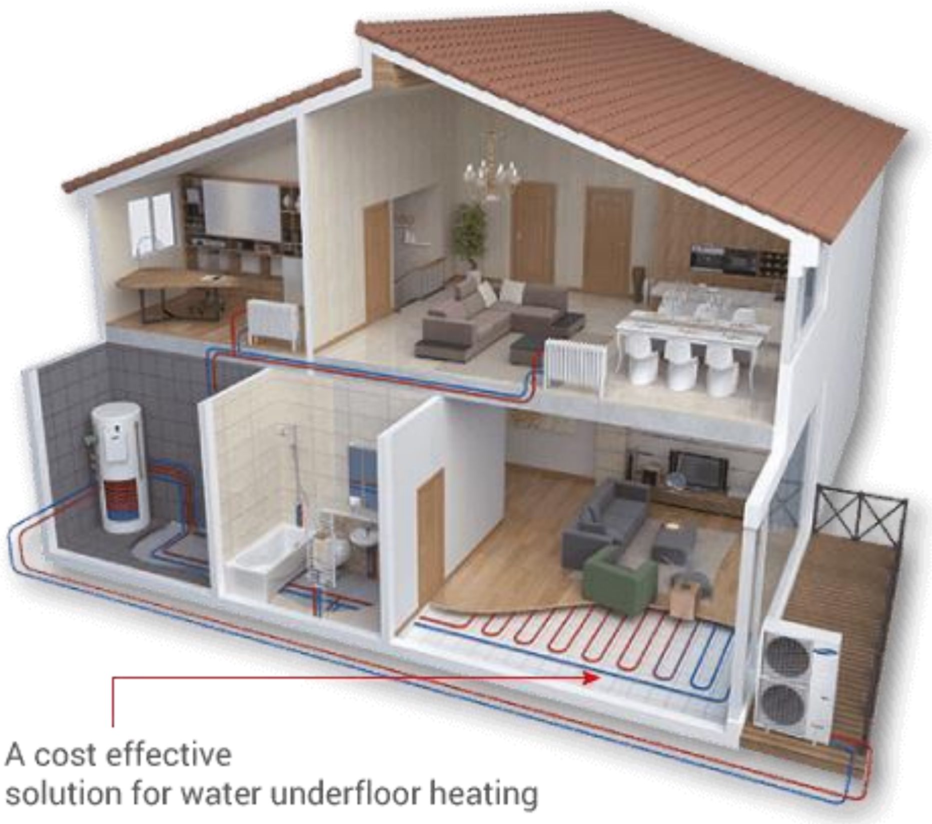

Picture 2.11. – Possibilities of heat pump air/water use [3]

2.6.2. Heat pump water/water

This type of heat pump can extract heat from a flowing source of low temperature water and deliver that heat to another, higher temperature water stream. The low temperature source may be ground water, cooling water from an industrial process or even process water that needs to be chilled before use. Almost any situation where heat is available in the form of low temperature water, in combination with a simultaneous load to which heat can be delivered in the form of higher temperature water, is a possible application for a water-to-water heat pump (Picture 2.12). [40]

Advantages:

- higher efficiency with CoP of around 5 – compared with other heat pumps;
- quick financial payback – less than 5 years for domestic;
- no boreholes and large trenches;
- low energy consumption;
- small carbon footprint. [37]

Disadvantages:

- lower components lifetime for pumping ground water (pumps, filters);
- higher service cost;
- use only in location with a plenty groundwater. [37]

Picture 2.12. – Heat pump water/water [36]

2.6.3. Heat pump ground/water

Ground source heat pumps (GSHP) extract heat from the ground by circulating fluid through buried pipes in *horizontal trenches* or *vertical boreholes*. They concentrate heat by using a vapour compression cycle, and they transfer heat into buildings to provide heating and hot water without burning fossil fuels. [19]

An investment in a GSHP system is an investment for the long term – the groundworks have a design life of 100 years and the GSHP itself has a life longer than any combustion boiler. [19]

2.6.3.1. Horizontal trenches

In the horizontal mode of the earth-coupled system, pipes are buried in trenches spaced a minimum of 1.5 m apart and from 1.2 – 2 m deep (Picture 2.13.). This allows for minimum thermal interference between pipes; however, this system is affected by solar radiation. A heat exchanger transfers heat between the refrigerant in the heat pump and the antifreeze solution in the closed loop. [50]


Picture 2.13. – Horizontal ground source heat pump [42],

The horizontal collector can be connected in way of slinky-loop, in spiral way and in meander way. This fact is described in the Picture 2.14.. [16]

1. Slinky-loop – is suitable for placement in flooded subsoil, where is high moisture concentration. Disadvantage of this type is great heat collection, relatively from small area and it causes local cooling of the subsoil.
2. Spiral – evenly extract of heat from area.
3. Meander – ideally spread extract of heat. Advantage of this type is that from the heat pump flows a cooler liquid and after passing through the meander, the warmest liquid is collected to the heat pump.

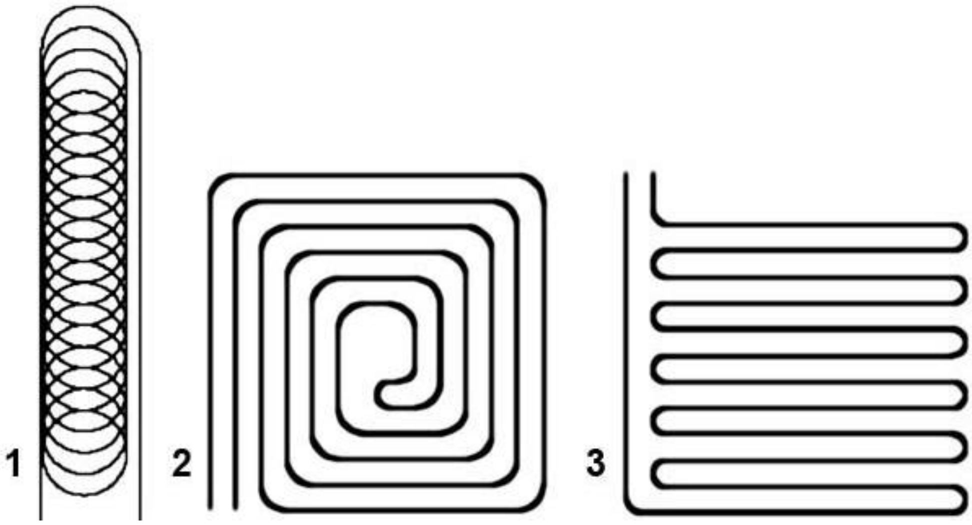

Picture 2.14. – Three types of horizontal collector connection [20]

Table 2.1. – Guidelines values to design the ground collector [31]

SUBSOIL	POSSIBLE HEAT COLLECTION	
	for 1 800 hours of operation	for 2 400 hours of operation
Dry frictional soil	10 W/m^2	8 W/m^2
Watered gravels and sand	20 - 30 W/m^2	16 - 24 W/m^2
Underground water, gravels and sand	40 W/m^2	32 W/m^2

2.6.3.2. Vertical boreholes

A ground source heat pump borehole represents a closed loop system which comprises a set of polyethylene pipes that are vertically inserted into the ground and which circulate water to and from the geothermal heat pump (Picture 2.15). In most cases, the borehole size will range between 15 and 122 m deep. [16]

The ground source heat pump boreholes are drilled at 5-6 m apart from each other and at 6-7 m from the nearest building. The depth is conditional on the property's characteristics (size, insulation and heating capacity) that require heating. A house that needs around 10 kW of heating capacity, most probably will need three boreholes of 80-110 m deep. [16]

Picture 2.15. – Vertical boreholes solution [16]

2.6.4. Seasonal performance factor

The Seasonal Performance Factor (SPF) only applies to heat pumps. It is a measure of how efficiently the heat pump is operating. Put simply, the higher SPF value the more energy efficient system is. SPF is a measure of the operating performance of an electric heat pump heating system over a year. It is ratio of the heat delivered to the total electrical energy supplied over the year. [22]

2.6.5. Coefficient of performance

The efficiency of refrigeration system and the heat pumps is denoted by its Coefficient of Performance (COP). The COP is determined by the ratio between energy usage of the compressor and the amount of useful cooling at the evaporator (for a refrigeration installation) or useful heat extracted from the condenser (for a heat pump). A high COP represents a high efficiency. [22]

The efficiency of the heat pump, COPh, depends on several factors. Especially the temperature difference between waste heat source and potential user is an important factor. The temperature difference between condensation and evaporation temperature mainly determines the efficiency, the smaller the difference, the higher the COPh. The Charts 2.3. bellow shows the influence of this temperature difference on the COPh value. The chart shows an increase in COPh with an increasing evaporation temperature. [22]

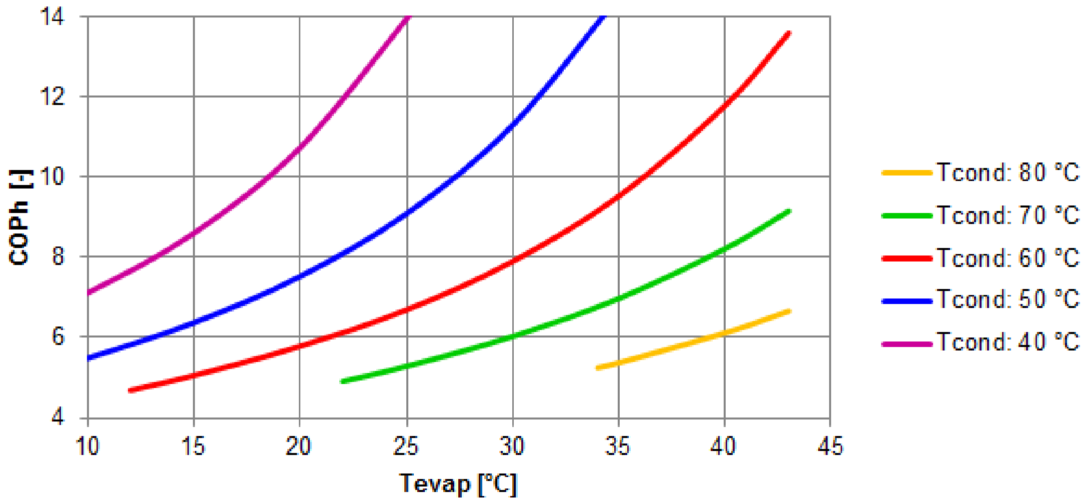

Chart 2.3. - Influence of the temperature difference on the COPh value [22]

2.6.6. Refrigerant

Is substance or mixture, usually fluid, used in heat pump and refrigeration cycle. In most cycles it undergoes phase transition from liquid to a gas and back again. Refrigerants are divided into three groups according to their chemical composition: HFCs, HCFCs and CFCs. [43]

HFCs = HydroFluoroCarbons are refrigerants that contain no chlorine and are not harmful to the ozone layer. HydroFluorCarbons are stron greenhouse gases and are regulated by the Kyoto Protocol – a 1997 international treaty to solve a global warming by curtailing emissions of greenhouse gases. However, their impact on the global warming is very large compared with traditional refrigerants. The most common HFCs refrigerants are shown in the Picture 2.16.. [43]

Picture 2.16. – HFCs refrigerants [2]

HCFCs = HydroChloroFluoroCarbons; the slow phase-out of CFCs shows it is a costly process. However, and more importantly, it also shows the problems and indecisiveness surrounding the availability of HCFCs, which were officially indicated as a temporary (until 2030) substitute for CFCs. [2]

The HCFCs contain less chlorine than CFCs, which means a lower ODP – Ozone Depleting Potential (factor indicating a substance´s relative ozone damaging power). Examples of HCFCs refrigerants is possible to see in the Picture 2.17.. [43]

Picture 2.17. – HCFCs refrigerants [2]

CFCs = ChloroFluoroCarbons are refrigerants that contain chlorine. They have been banned since the beginning of the 90´s because of their negative environmental impacts. Examples of CFCs are R11, R12 and R115. The conversion of equipment and systems using CFCs has no yet been completed. On the contrary, the illegal market for this type of refrigerants flourishes worldwide, and it is estimated that no more than 50 % of CFC system worldwide have been upgraded. The types of CFCs refrigerants is possible to see in the Picture 2.18.. [43]

Picture 2.18. – CFCs refrigerants [2]

3. CALCULATION PART

This chapter describes formulas that are used in project part of master´s thesis for calculation and evaluation of data.

3.1. DIAGNOSTIC OF EXTERNAL AND INTERNAL BOUNDARY CONDITIONS OF GROUND HEAT DISTRIBUTION IN SPA

The sources of high-potential thermal energy are hydrothermal sources – thermal waters, heated due to the geological processes. It is necessary to determine various factors when designing a ground heat exchanger in the geothermal fields that affect the efficiency of heat transfer and heat recovery.

3.1.1. Thermal conductivity of saturated soil

Saturation and dry density are important parameters governing soil thermal conductivity. An increase in either saturation or dry density of a soil will result in an increase in its conductivity. Both of these parameters should be accounted for in conductivity prediction methods, defined by: [5]

$$\lambda(S) = K_e.\left(\lambda_{sat} - \lambda_{dry}\right) + \lambda_{dry} \qquad (3.1.)$$

Where:

λ (S)	thermal conductivity at saturation S (W.m^{-1}.K^{-1})
K_e	normalized thermal conductivity (W.m^{-1}.K^{-1})
λ_{sat}	thermal conductivity of saturated soil (W.m^{-1}.K^{-1})
λ_{dry}	thermal conductivity of dry soil (W.m^{-1}.K^{-1})

At full saturation, a soil has only two phases, water and soil grains. To estimate λ_{sat}, Johansen proposed a geometric mean based on the λ of two phases:

$$\lambda_{sat} = \lambda_s^{1-\phi}.\lambda_w^{\phi} \qquad (3.2.)$$

In these expressions:

λ_w	thermal conductivity of water (W.m^{-1}.K^{-1})
ϕ	porosity (%)
λ_s	effective thermal conductivity of soil solids (W.m^{-1}.K^{-1})

$$\lambda_s = \lambda_q^{q}.\lambda_0^{1-q} \qquad (3.3.)$$

Where:

q	quartz content of the total solids (%)
λ_q	thermal conductivity of quartz ($W.m^{-1}.K^{-1}$)
λ_0	fraction of other minerals ($W.m^{-1}.K^{-1}$)

For estimating λ_{dry} Johansen developed a semiempirical relationship:

$$\lambda_{dry} = \frac{0.135\,.\ \rho_b\ +\ 64.7}{\rho_s\ - 0.947.\rho_b} \tag{3.4.}$$

Where:

ρ_b	dry bulk density ($kg.m^{-3}$)
ρ_s	average density of the soil solids ($kg.m^{-3}$)

Recently, Côté and Konrad (2005) improved the method of Johansen (1975) and proposed a generalized K_e-S relationship valid for all soils based on experimental investigations on pavement base-course and sub-base materials: [5]

$$K_e = \frac{\kappa S}{1 + (\kappa - 1)S} \tag{3.5.}$$

Where:

κ	dimensionless empirical fitting parameter (-)

3.1.2. Heat transfer in porous media

The temperature equation defined in porous media domains corresponds to the convective-diffusion equation with thermodynamic properties averaging models to account for both solid matrix and fluid properties: [21]

$$(\rho C_p)_{eff} \frac{\partial T}{\partial t} + \rho C_p u\,.\nabla T +\ \nabla\,.\,q = Q \tag{3.6.}$$

The different quantities appearing here are:

ρ	fluid density ($kg.m^{-3}$)
C_p	fluid heat capacity at constant pressure ($J.kg^{-1}.K^{-1}$)
$(\rho C_p)_{eff}$	effective volumetric heat capacity at constant pressure ($J.m^{-3}.K^{-1}$)
k_{eff}	effective thermal conductivity ($W.m^{-1}.K^{-1}$)
q	conductive heat flux ($W.m^{-2}$)

u	velocity field (m.s $^{-1}$)
Q	heat source (W.m $^{-3}$)

Fourier´s law of heat conduction states that the conductive heat flux, q, is proportional to the temperature gradient, ∇T:

$$q = -k_{eff} \, . \nabla T \tag{3.7.}$$

This equation is valid only when the temperatures into the porous matrix T_s and the fluid T_f are in equilibrium – local thermal equilibrium:

$$T_f = T_s = T \tag{3.8.}$$

3.1.3. Darcy´s Law

One application of Darcy´s law is to water flow through an aquifer. It is a phenomenological derived constitutive equation that describes the slow flow of a fluid through a porous medium, defined by: [4]

$$\frac{\partial}{\partial t}\left(\epsilon_p \rho\right) \nabla . (\rho u) = Q_m \tag{3.9.}$$

Where:

ε_p	pororsity (%)
ρ	fluid density (kg.m $^{-3}$)
u	Darcy velocity (m.s $^{-1}$)
Q_m	heat source (W.m $^{-3}$)

Darcy velocity u in a porous medium is calculated from hydraulic conductivity and the head gradient:

$$u = -\kappa . \frac{\Delta H}{\Delta L} \tag{3.10.}$$

Where:

κ	hydraulic conductivity (m.s $^{-1}$)
ΔH	difference in hydraulic head between two lateral points (m)
ΔL	distance between two lateral points (m)

3.2. ANALYSIS OF BOUNDARY CONDITIONS OF THE GROUND HEAT EXCHANGERS

This chapter content information about physical processes, as well as various equations and boundary conditions that must be solved for the invent of ground heat exchangers, including thermodynamic and fluid dynamic design. All around is a complex process involving the integration of design rules and empirical knowledge from several areas, especially for the horizontal ground heat exchanger that present complex characteristics of heat transfer and thermal-hydraulic parameters.

3.2.1. Heat transfer in pipes

The energy equation for an incompressible fluid flowing in a pipe is:

$$\rho A C_p \frac{\partial T}{\partial t} + \rho A C_p u e_t . \nabla T = \nabla . AkT + f_D . \frac{\rho A}{2 d_h} |u|^3 + Q + Q_{wall} \qquad (3.11.)$$

Where:

ρ	density (kg.m $^{-3}$)
A	pipe cross section area (m ^{2})
C_p	fluid heat capacity at constant pressure (J.kg^{-1}.K^{-1})
T	temperature (K)
f_D	Darcy friction factor (-)
d_h	hydraulic diameter (m)
u	tangential velocity (m.s $^{-1}$)
k	thermal conductivity (W.m^{-1}.K^{-1})
Q	general heat source (W.m $^{-1}$)
Q_{wall}	external heat exchange through the pipe wall (W.m $^{-1}$)

Unit tangent vector e_t describes velocity, in which direction is moving. This fact is illustrated bellow in the Picture 3.1.

Picture 3.1. – Unit tangent vector to the pipe axis [54]

$$e_t = (e_{t,\ x};\ e_{t,\ y};\ e_{t,\ z}) \qquad (3.12.)$$

The radial heat transfer from the surroundings into the pipe is given by equation:

$$Q_{wall} = (hZ)_{eff}.\Delta T \quad (3.13.)$$

Where:

h	heat transfer coefficient ($W.m^{-2}.K^{-1}$)
Z	wall perimeter (m)
ΔT	temperature differences across the wall (K)

The overall heat transfer coefficient including internal film resistance, wall resistance and external film resistance can be deduced as follows, with reference to Picture 3.2..

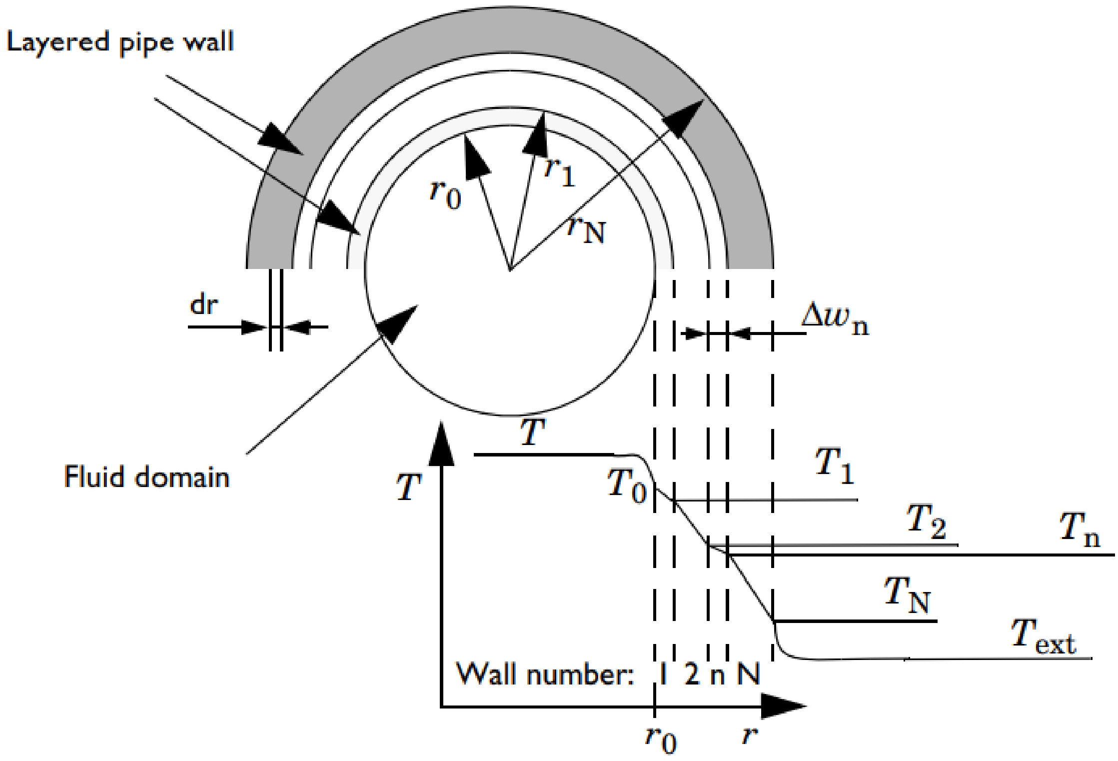

Picture 3.2. – Temperature distribution across the pipe wall [34]

In the Picture 3.2., the different quantities appearing:

r_n	outer radius of wall *n* (m)
$w = r - r_0$	a wall coordinate (m) – starting at the inner radius r_0
$\Delta w_n = r_n - r_{n-1}$	the wall thickness of wall *n* (m)
Z_n	outer perimeter of wall n
h_{int}	heat transfer coefficient on the inside of the pipe ($W.m^{-2}.K^{-1}$)
h_{ext}	heat transfer coefficient on the outside of the pipe ($W.m^{-2}.K^{-1}$)
k_n	thermal conductivity of wall *n* ($W.m^{-1}.K^{-1}$)

The effective value $(hZ)_{eff}$ of the heat transfer coefficient and wall perimeter of the pipe for circular cross section is calculated by equation:

$$(hZ)_{eff} = \frac{2\pi}{\frac{1}{r_0 h_{int}} + \frac{1}{r_N h_{ext}} + \sum_{n=1}^{N} \left(\frac{\ln\left(\frac{r_n}{r_{n-1}}\right)}{k_n} \right)} \tag{3.14.}$$

3.2.1.1. <u>Pipe properties</u>

For the calculations mentioned above, it is necessary to define the basic boundary conditions of the pipeline and its properties, for example: pipe shape, friction resistance, hydraulic diameter, Reynolds number, etc.

Darcy friction factor f_D for single-phase fluids it is expressed by Churchill equation:

$$f_D = 8\left[\left(\frac{8}{Re}\right)^{12} + (c_A + c_B)^{-1,5}\right]^{\frac{1}{12}} \tag{3.15.}$$

Where:

$$c_A = \left[-2,457\, ln\left(\left(\frac{7}{Re}\right)^{0,9} + 0,27\left(\frac{e}{d_h}\right)\right)\right]^{16} \tag{3.16.}$$

$$c_B = \left(\frac{37530}{Re}\right)^{16} \tag{3.17.}$$

$$Re = \frac{\rho u d_h}{\mu} \tag{3.18.}$$

Re	Reynolds number (-)
c_A	A contribution (-)
c_B	B contribution (-)
e	surface roughness (m)
d_h	hydraulic diameter (m)
μ	fluid dynamic viscosity ($kg.m^{-1}.s^{-1}$)
ρ	fluid density ($kg.m^{-3}$)
u	flow velocity ($m.s^{-1}$)

4. PROJECT

The subject of this chapter is application of calculation methods to the part of ground heat exchangers in the spa, numerical analysis of heat transfer in the ground with horizontal exchanger, elaboration of solutions to increase heat transfer effectivity and description of created schemes and solutions. Simulation calculations by using software COMSOL Multiphysics 5.6. allowed to determine long-term temperature changes at various depths of the ground, related to the operation of the ground heat exchanger. This software work within the finite element method (FEM) framework.

4.1. CONSIDERATION FACTORS

The ground is the most widespread source of renewable energy. Heat pumps that use the ground as a heat source or sink are called ground-source heat pumps (GSHP). This system is complicated and can be unpredictable too. The process of mapping and modelling the system is a long and never ending.

Due to the difficulty of accessing GSHP after they installation, materials and assembling quality must satisfy the very high requirements. One of the primary problems of the construction GSHP is the calculation of heat power which collector can throw down into the ground – cooling mode, or absorb from the ground – heating mode.[38]

The real heat power depends on several factors:

- thermo-physical properties of soil;
- climatic conditions;
- depth of GSHP;
- collector construction;
- material properties of collector.

As most important boundary conditions in many engineering project as well as to design ground heat exchanger is the characteristic of subsoil, respectively its thermal properties. The problem of heat transfer in soils is very complicated and to understand it one must subdivide it into its constituent elements and facets.

Every part of landscape has various types and several layers compositions, it means, different properties. Temperature and water content in soils has a big effect to determine thermo-physical properties, for example: thermal conductivity and heat capacity. Common values of thermal conductivity, diffusivity and specific heat and of different soils and their phase components are summarized in Table 4.1. To elaborate the master´s thesis I chose Slovak Republic as it is a very interesting country from a geothermal point of view.

Table 4.1. – Thermal properties of common components in soil [11]

Material	Density ($kg.m^{-3}$)	Heat capacity ($kJ.kg^{-1}.K^{-1}$)	Thermal conductivity ($W.m^{-1}.K^{-1}$)	Thermal diffusivity ($(m^2.s^{-1}).10^{-7}$)
Air (10 °C)	1.25	1.000	0.0026	0.21
Water (25 °C)	999.87	4.200	0.56	1.43
Water vapor (1 atm, 400 K)	x	1.901	0.016	233.8
Ice (0 °C)	917	2.040	2.25	12
Quartz	2.660	0.733	8.40	43.08
Granite	2.750	0.890	1.70-4.00	12
Gypsum	1.000	1.090	0.51	4.7
Limestone	2.300	0.900	1.16-1.33	5
Marble	2.600	0.810	2.80	13
Mica	2.883	0.880	0.75	2.956
Clay	1.450	0.880	1.28	10
Sandstone	2.270	0.710	1.60-2.10	10-13

4.2. LOCATION OF INTEREST

The advantage of Slovakia is that the natural heating water is present naturally under the ground, but is vastly used for recreation this time. There are 116 registered geothermal wells with temperatures ranging between 18 °C – 129 °C. Slovak territory is essentially illustrated in the Picture 4.1., shows depict activity of natural healing water in determined areas. [15]

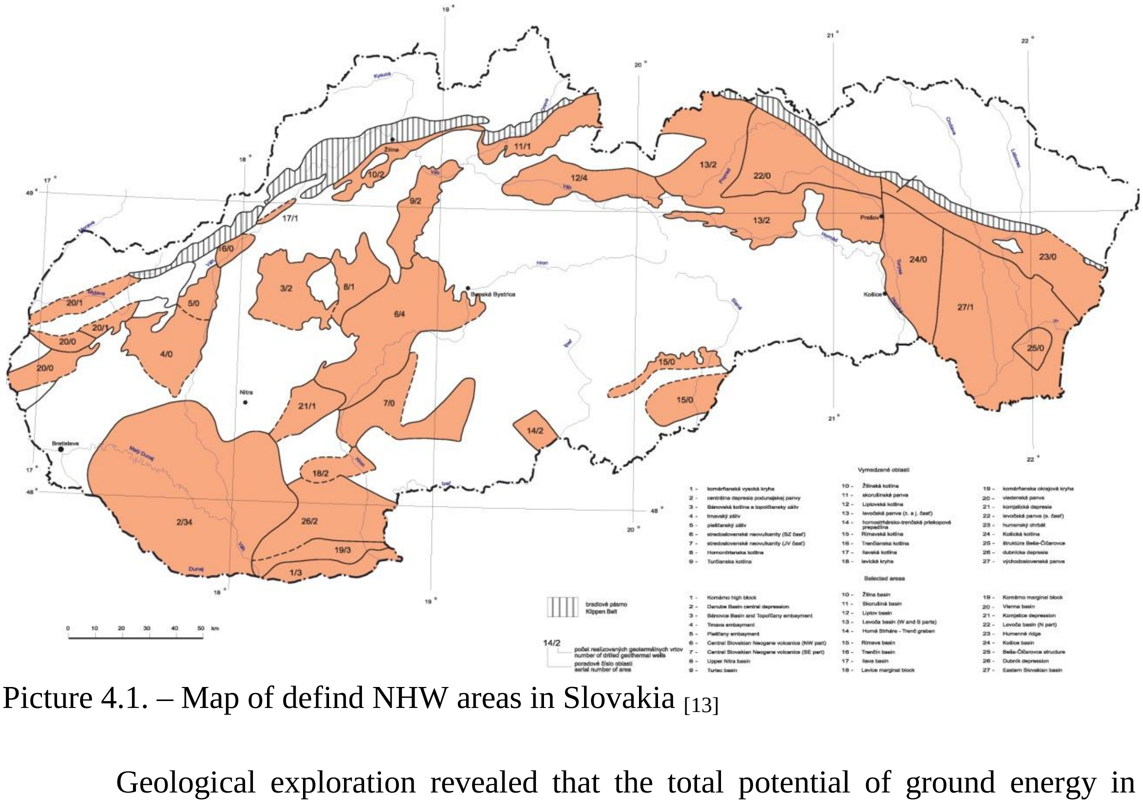

Picture 4.1. – Map of defind NHW areas in Slovakia [13]

Geological exploration revealed that the total potential of ground energy in Slovakia is approximately 5 500 MW of which only 131 MW is currently utilized for heating. [44]

4.2.1. Spa Island Piešťany

For the purpose of this master´s thesis elaboration due to its size of issues it will be aimed only on chosen part of Slovak Health Spa Island in Piešťany that it is illustrated bellow in the Picture 4.2.

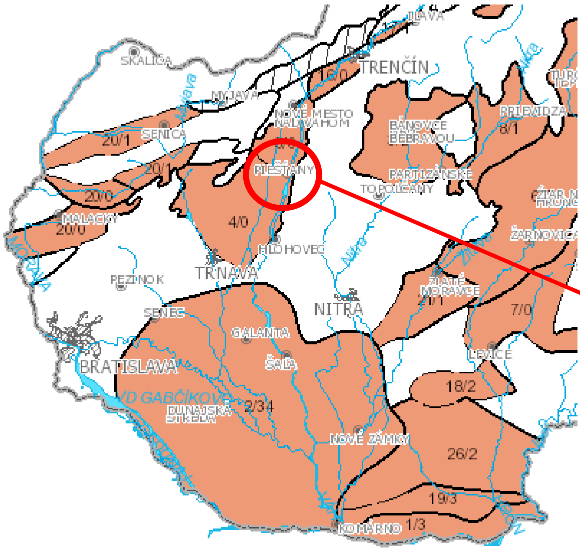

Picture 4.2. – Spa Island location [27]

The Spa Island is one of Europe´s largest and most unique spa complexes with long-term use of mineral water resources of mineralization about 1 200 – 1 400 $mg.l^{-1}$. The water type is SO_4 with high content of sulphide 4-10 $mg.l^{-1}$ and unique sulphur mud formation. These waters have permeated the limestone for many centuries and have been naturally heated by Earth´s magma to temperatures within 67 – 69 °C. [9]

4.3. GEOLOGICAL CHARACTERISTIC OF THE STUDY TERRITORY

Interest area is created by quaternary sediments that are represented by river alluviums from river Váh, that are covered by 1 – 3 m layer of watery clay. The clay contains sandy admixture and smaller amount of pebble. In some place above this water clay layer is made up ground layer. Sand-gravel alluviums from Váh of different thicknesses within the range 6 m – 12 m are placed under clay blanket. This thickness of sand-gravel sediments is dependent on non-flat surface that was broken by erosive gully. [39]

In the subsoil of quaternary sediments is placed a neogene, which is formed by fine-grained to medium-grained sediments at the surface. The water creates a groundwater stream with free level in sand-gravel alluviums. [39]

The subsoil of quaternary materials creates relatively impermeable neogene sandstone, which contain caolinic sealant. Common groundwater is mixed with natural healing water that goes through the breaks, as it is possible to see in the Picture 4.3., from considerable depths from mesozoic carbonate rocks. [39]

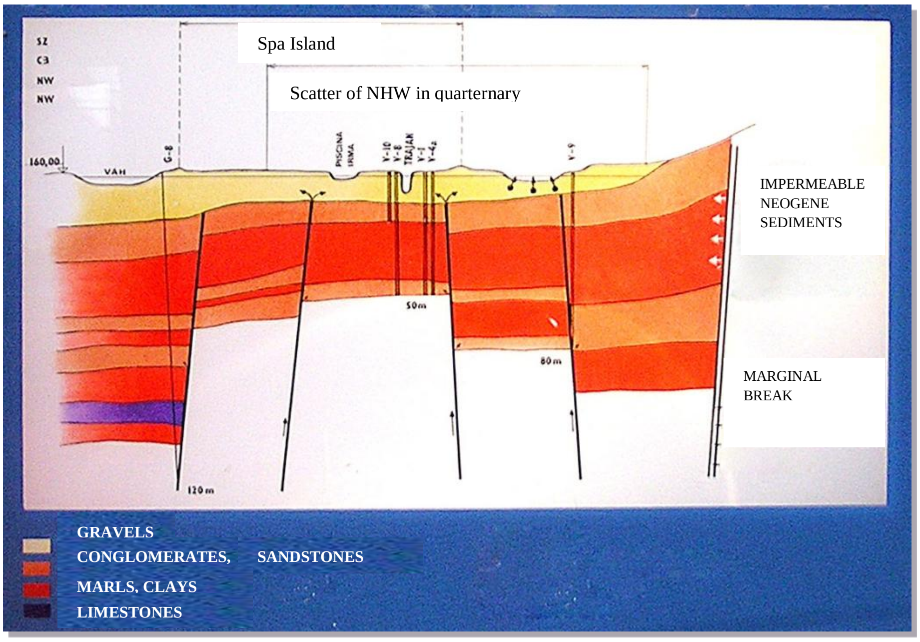

Picture 4.3. – Scheme of spring area construction [Source: Archive of SLKP a.s.]

4.3.1. Soil composition

Soil as a multi-phase material consisting of solid particles, gas or liquid and each type and different content of solid particles or water change thermal properties of the soil. For heat transfer computation whether analytical or numerical it is necessary to know exact thermal conductivity as a main component. In isotropic homogeneous medium is for a given rock a constant, which characterizes the ability of the rocks to conduct heat.

The Spa Island is usually dominated by clay, gravel, loam, limestone, sand and sandstone. In software COMSOL Multiphysics 5.6. was created simplified three-dimensional model of subsoil layers that is illustrated in the Picture 4.4., based on the composition and depth according the Table 4.2.

Table 4.2. – Soil composition in the Spa Island

Depth	Soil composition
0,00-1,60	Loam
1,60-2,60	Coarse gravels with sand, thickly clayey
2,60-3,30	Coarse gravels with sand, weakly clayey
3,30-4,20	Coarse gravels up to Ø10 cm
4,20-6,30	Sandstone with putty of thermal salts
6,30-9,00	Coarse gravels up to Ø12 cm

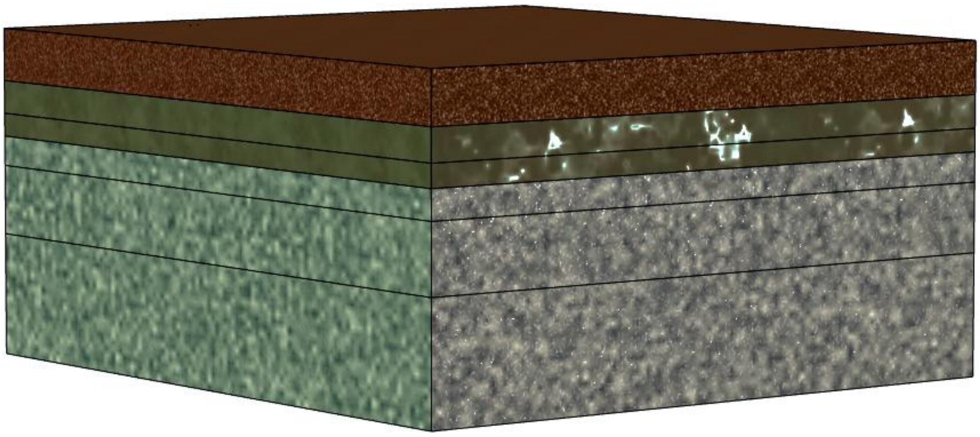

Picture 4.4. – Illustration of simplified soil composition

Numerical modelling related to heat transfer in subsurface was divided in two foremost physical interfaces, that it is illustrated in the Picture 4.5.:

1. Heat transfer in porous medium
    - Solid layer
    - Porous medium
2. Heat transfer in pipe

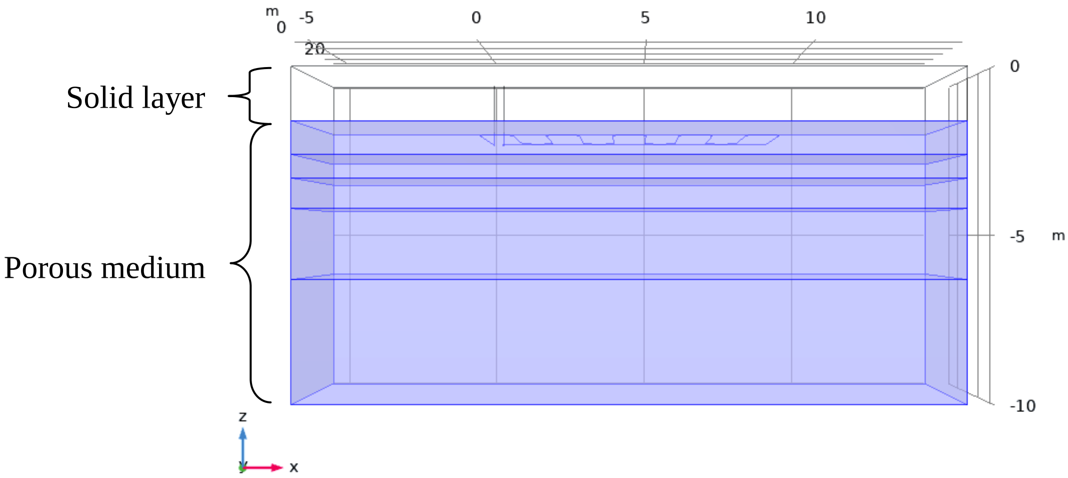

Picture 4.5. – Subsurface division from physical point of view

4.3.2. Saturated and unsaturated soil comparison of thermal conductivity

Thermal conductivity coefficient values of soil are useful in many subjects connected with energetic. This parameter is defined as the quantity of heat transmitted through a unit thickness in a direction normal to a surface of unit area due to a unit temperature gradient under steady state conditions. The objective of this study is thermal conductivity comparison and evaluation of saturated soil and unsaturated soil for the case study.

Previous researches have shown that thermal conductivity is affected by many factors, as a:

- water content;
- temperature;
- porosity;
- dry density;
- mineral composition;
- degree of saturation;
- particle size.

Based on the studies and physics is given that thermal conductivity of soil increases with increasing moisture content. As an example Table 4.3., that is illustrated bellow, shows range of different soil type thermal conductivity from dry to saturated soil.

Table 4.3. – Thermal conductivity range for various soil types [45]

Soil type	Thermal conductivity λ [W.m^{-1}.K^{-1}]
Sandy loam	0.37 – 1.42
Loam	0.37 – 1.90
Sandy clay	0.38 – 1.71
Clay	0.39 – 0.41

There is no simple and general relationship between the thermal conductivity of a soil, λ, and its volumetric water content, θ, because the porosity, n, and the thermal conductivity of the solid fraction λ_s play a major part. [48]

Thermal conductivity calculation method for saturated soils was established by scientist Johansen (1975) and by Côté and Konrad (2005, 2009), that is described in calculation part of the thesis. The method proposed by Johansen uses an interpolation approach to estimate the λ of soil at a given saturation S based on the dry and saturated soil thermal conductivities. [48]

Water content at temperature of 50 °C, determine the relative change of thermal conductivity between thermal conductivity of dry and saturated clay. This study developed a comprehensive thermal conductivity value is estimated as a one of the boundary condition for precisely numerical simulation. In the Table 4.4. bellow, the input data for thermal conductivity calculation of saturated soil as a porosity, quartz content, thermal conductivity of quartz, thermal conductivity of water, bulk density, mean density, intermediate degree of saturation and results are stated. Computation procedure is described in CHAPTER 3. – CALCULATION PART. The result value of saturated soil of porosity 0,4 is 1,4820 W.m^{-1}.K^{-1}.

Table 4.4. – Thermal conductivity calculation for saturated strata

Input data	Results
$\lambda_w = 0.6485\ W.m^{-1}.K^{-1}$ thermal conductivity of water at 50 °C	$\lambda_{sat} = 1.3183\ W.m^{-1}.K^{-1}$ thermal conductivity of saturated soil
$\phi = 40\ \% = 0.4$ porosity	
q = 5 % = 0.05 quartz content	$\lambda_s = 2.1155\ W.m^{-1}.K^{-1}$ effective thermal conductivity of soil solids
$\lambda_q = 6.15\ W.m^{-1}.K^{-1}$ thermal conductivity of quartz	
$\lambda_0 = 2.0\ W.m^{-1}.K^{-1}$ fraction of other minerals	
$\rho_b = 1.28\ g.cm^{-3} = 1\ 280\ kg.m^{-3}$ bulk density	$\lambda_{dry} = 0.1652\ W.m^{-1}.K^{-1}$ thermal conductivity of dry soil
$\rho_s = 2.65\ g.cm^{-3} = 2\ 650\ kg.m^{-3}$ mean density	
$\kappa = 1.45$ intermediate degree of saturation	$K_e = 1.1420$ Kersten number
$\mathbf{\lambda(S) = Ke\ .\ (\lambda_{sat} - \lambda_{dry}) + \lambda_{dry} = 1.4820\ W.m^{-1}.K^{-1}}$	

4.4. CLIMATIC CONDITIONS

Temperature regime of the soil surface layers of the Earth is formed under the influence of two basic factors – solar radiation falling on the Earth´s surface and radiogenic heat from inside the Earth. Seasonal and daily changes in the intensity of solar radiation and the air temperature cause fluctuations in the temperature of subsurface layers. The penetration depth of the daily fluctuation of the air temperature and the intensity of the incident solar radiation does not usually exceed 15 – 20 m.

Slovakia climate can be described as typical European continental influenced climate with warm, dry summers and fairly cold winters. Due to landscape variations, climate in Slovakian lowlands is warmer than in mountains and altitude is similarly applied to climatic seasons. The warmest part includes Danubian Lowland and Eastern Slovak Lowland. This fact is shown in the Picture 4.6. [35]

Piešťany and its surroundings are among the warmest areas in Slovakia. The climate is typically lowland, slightly dry and slightly wind. The nearby mountains direct flow, direction and speed. It belongs to the climatically-geographic type of lowland area mostly warm. The average annually air temperature reaches 9,2 °C and total annual rainfall is up to 600 mm. [33]

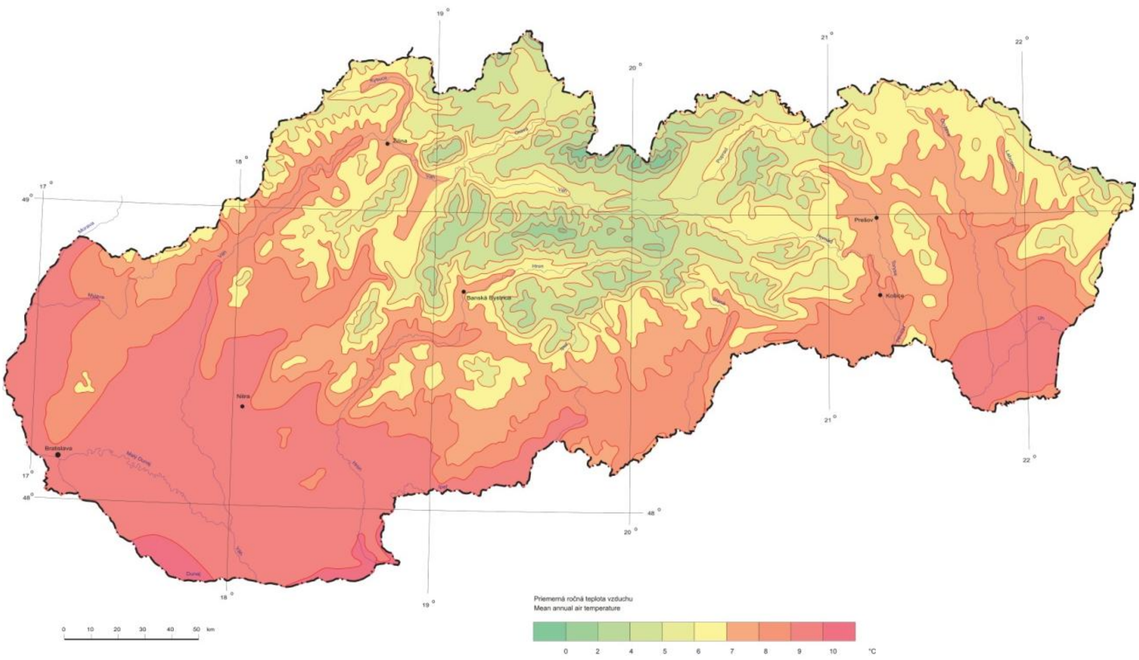

Picture 4.6. – Average annual air temperature in Slovakia [13]

Data used for the brief assessment of climatic conditions are drawn from Slovak Hydrometeorological Institute and subsequently processed into a chart that is illustrated bellow as a Chart 4.1.

This developed chart, using Piecewise interpolation, falls on 10 years of measured data for mean monthly air temperature in Piešťany. Is it possible to see that the warmest month is July with average air temperature 21,9 °C and the coldest one is January with average air temperature - 2,7 °C. Total average air temperature for the last 10 years is 10,8 °C. These data were used within the elaboration of numerical simulation for ground heat exchanger as a boundary condition. The precipitations are neglected.

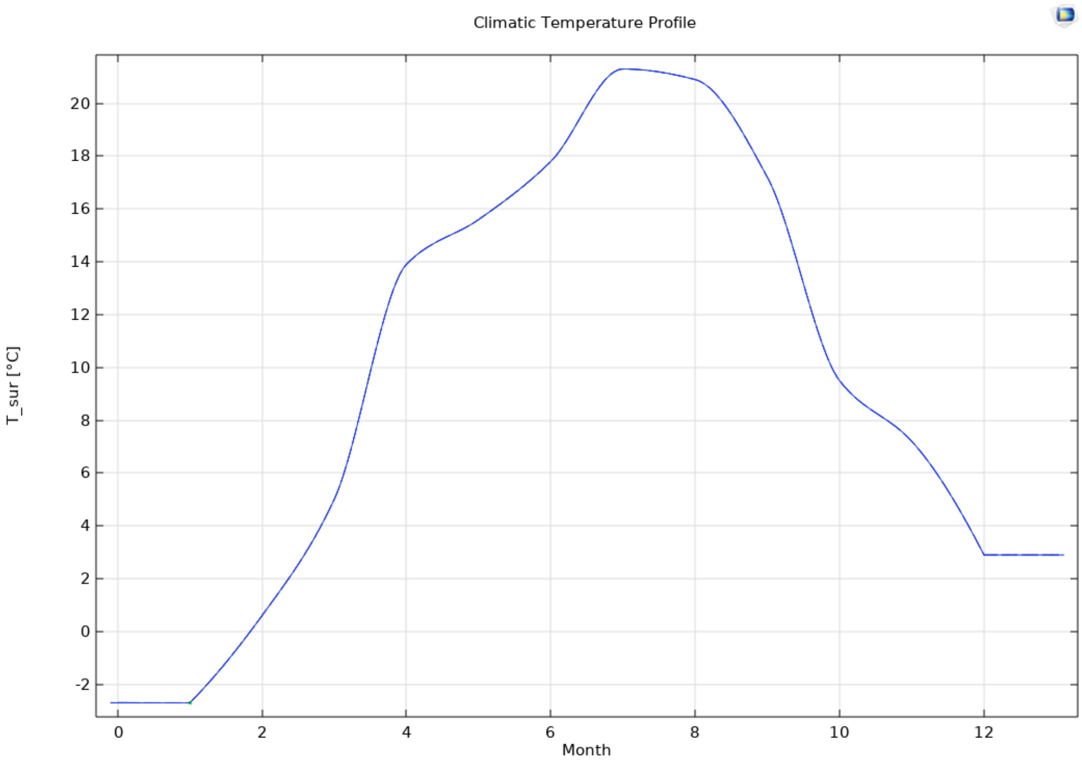

Chart 4.1. – Average annual air temperature for location of interest

4.5. TEMPERATURE CONDITIONS

Thermal energy in the earth is distributed between the constituent host rock and the natural fluid that is contained in its fractures and pores. The ground is usually treated as a system consist of subsurface layer, in which there are interactions related to changing weather conditions and a deeper layer, in which these impacts do not occur.

As mentioned above, subsoil of Spa Island reaches temperatures up to 69 °C caused by NHW that goes through the breaks and under this natural condition, the ground is approximately immutable. This is called undisturbed ground temperature (UGT). Values of geothermal gradient real occurring in nature have only a minimal impact on UGT diversity and average ground temperature in this location. The temperature condition has been already investigated in the previous final thesis. As it is necessary to understand correctly how the temperature was determined and applied in the case study, therefore a brief description of the entire analysis with results are stated bellows.

4.5.1. Observation drills

In the Spa Island Piešťany was on 24. 10. 1955 – 17. 03. 1956 installed 54 pieces of observation drills. Drills were built-in on the way of well with gravel backfill, which exceeds the perforation length on each side 0,20 m and is protected on both sides by coarse layer of sand 0,20 m, against the ingress of clay soil to observation drills. [47]

In the situation map of Spa Island in Piešťany are plotted all observation drills of system A – Annex 8.1..

4.5.1.1. Evaluation of drill system

According to the temperature measurement results by thermistor thermometer is possible to assume, that even in the south-eastern part of thermal area scattering was mainly in the horizon upper part and then the values temperature shift will be more pronounced. [47]

The Annex 8.2. content a table which consist of the drill number, drill depth, temperature at the base and at the water level show that maximum temperature is 64,7 °C in depth 7,67 m at the base of drill A-18. [47]

Data were measured on 27. 03. 1956 during the afternoon hours. Due to electric current failure the pumps were not in operation at the well Trajan from 27. 03. 1956 until 28. 03. 1956. These values are no to affected by any artificial intervention.[47]

4.5.1.2. Temperature outputs

In 1965, temperatures in the observation drills of system A were again measured. Based on measured values, the drawings were experimentally created of Spa Island, which are shown by temperature isolines. For each of them were measured temperatures in months 5th, 6th, 7th, 8th, 9th, 10th, 11th, 12th.[44]

The drawings consist of the thermal isolines divided to 2 colours – blue one and red one. Each colour is characterized by different date of measurement. Next one what we can find in the drawings is water level of bypass river, drills of system A and D and named buildings. [14]

From obtained drawings – profiles from State Geological Institute of Dionýz Štúr I have created an interpolation tables depending on depth, length and temperature, which I subsequently transformed to the 2D thermal profiles. [14]

The all profiles was redraw in AutoCad , where grids was created with depths 2 m, 4 m, 6 m, 8 m and 10 m, and with different lengths. An interpolation table was done in Excel and then 2D thermal profile was subsequently developed. [14]

These temperature fields and drawings were created for the one part of my bachelor´s thesis to understand the conditions for the design of ground heat exchanger by numerical simulation as a main part of my master´s thesis and to determine boundary conditions for the temperature profile in the subsurface, and for design the exchanger in different effectivenesses.

4.5.2. Ground temperature field

The profile No. 1a consists of four main ground subsoil 2D thermal profiles. Two are processed for the summer and two for the winter. Temperature data for the profile creation in the summer were measured on 27. 07. 1965 (Chart 4.2. – the first profile) and on 24. 08. 1965 (Chart 4.2. – the second profile), for winter were measured on 29. 11. 1965 (Chart 4.3. – the first profile) and on 28. 12. 1965 (Chart 4.3. – the second profile). I chose the base point D18 – drill. The length of this profile is 500 m. The profiles are created in the following depths: 2 m, 4 m, 6 m, 8 m, and 10 m. [14]

Because these two seasons the profiles are influenced by outside temperatures, rainfalls and in case of winter by snow also was necessary determine stable and unstable temperatures in the ground subsoil by temperature differential. [14]

Maximal temperature: 55 °C
Minimal temperature: 15 °C

4.5.2.1. Summer season

Temperature difference between the months July and August is almost unchanged. The average temperatures during these two months are mentioned in the Chart 4.2. as a third profile. We can see in the two meters depth is temperature scattering of 55 °C already. Epicentre of the highest temperatures is collect in the length range from about 105 m – 255 m in depths from 2 m – 6 m and in depths from 8 m – 10 m is length range between 105 m – 270 m. [14]

4.5.2.2. Winter season

The temperatures are radically influenced during the months November and December by climatic conditions in comparison with summer months, especially in depth of 2 m – 4 m. In this case is maximal temperature 50 °C in two meters depth. However, the temperatures are increasing in 10 m depth from 50 °C to 55 °C and from 40 °C to 45 °C. This fact is shown in the Chart 4.3. in length range 130 m – 305 m . [14]

4.5.2.3. Temperature differential

In case of profile 1a the temperature difference between the summer and the winter season is mostly 0 °C – 5 °C (Chart 4.4.) Such a small thermal differential is in depths 6 m – 10 m due to it is not influenced by external conditions like a rainfalls, snow in global by outside temperature. Maximal temperature difference is 20 °C in depth 2 m of 10 m length and in depth 4 m of length 5 m only. [14]

4.5.3. Temperature determination

Based on these temperature profiles of ground subsoil we had determined the ground temperature into two variants. As a first one is low-potential place and as a second variant is high-potential place. At lower potential is considered temperature of 15 °C and at higher potential places is considered temperature up to 50 °C. It is necessary to know that considered temperatures at the lower potential and at the higher potential places are year-round stable.

Within the elaboration of the master thesis, temperature boundary condition is determined for high-potential place of 50 °C annually in two possible cases. The first possible case is that the subsoil temperature in the Spa Island is constant from 2 m depth up to 10 m. The temperature will be affected only from the surface to 2 m depth by the climatic conditions. The second possible case is to set a temperature of 50 °C as unstable temperature and investigate the impact of using ground heat exchanger in subsoil.

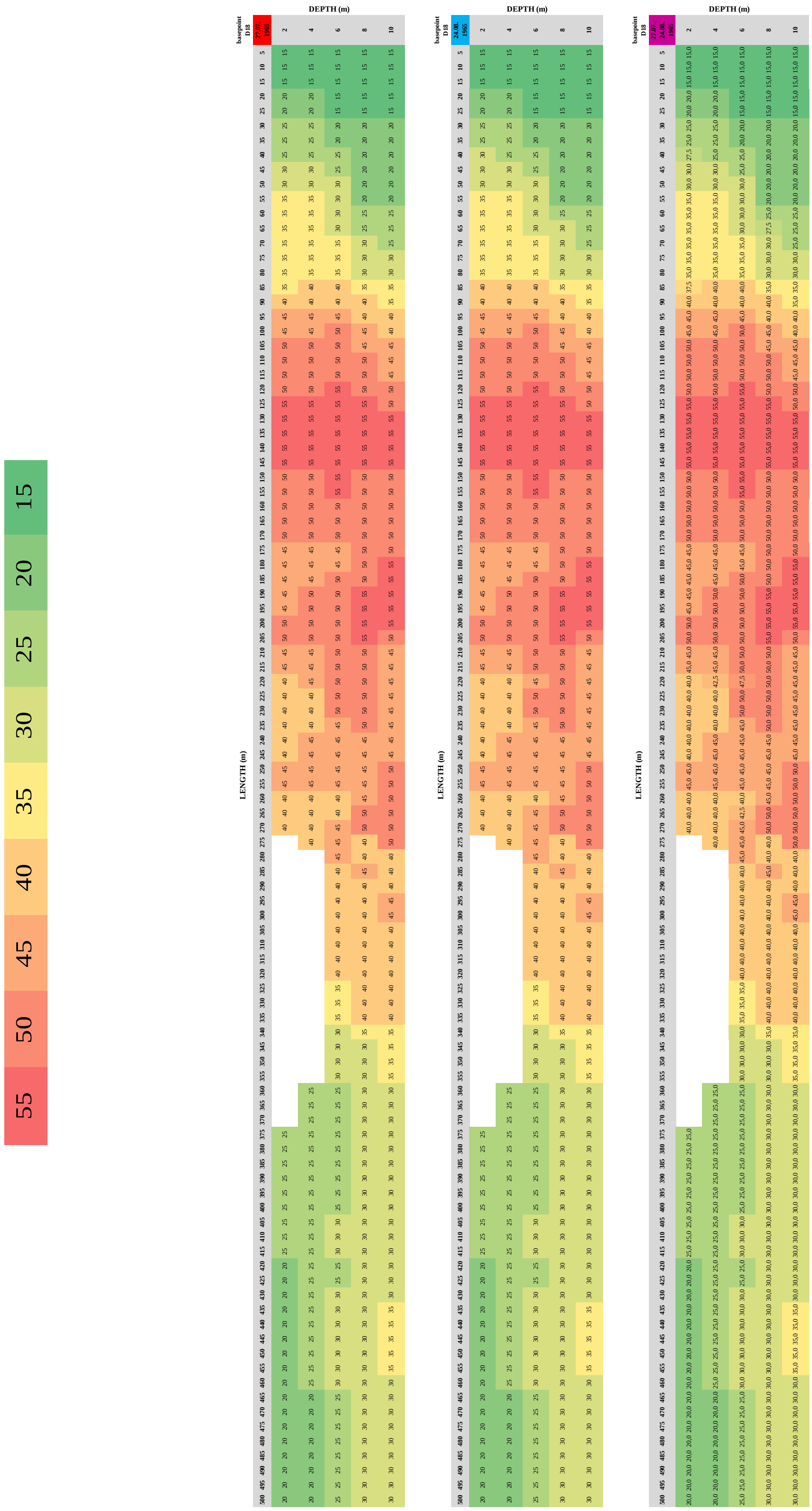

Chart 4.2. – Thermal fields of Spa Island No. 1a during the summer season and their average [14]

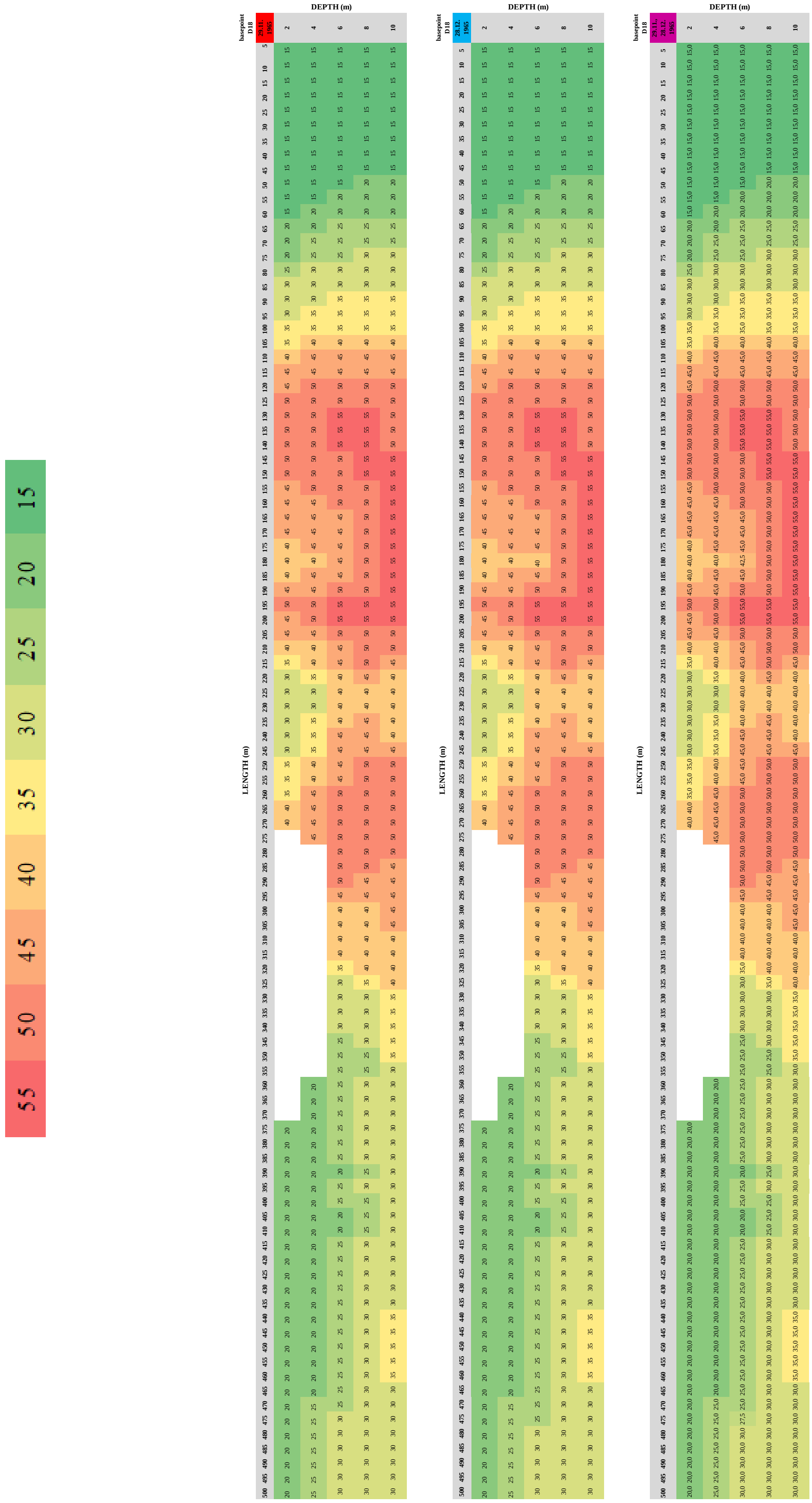

Chart 4.3. – Thermal fields of Spa Island No. 1a during the winter season and their average [14]

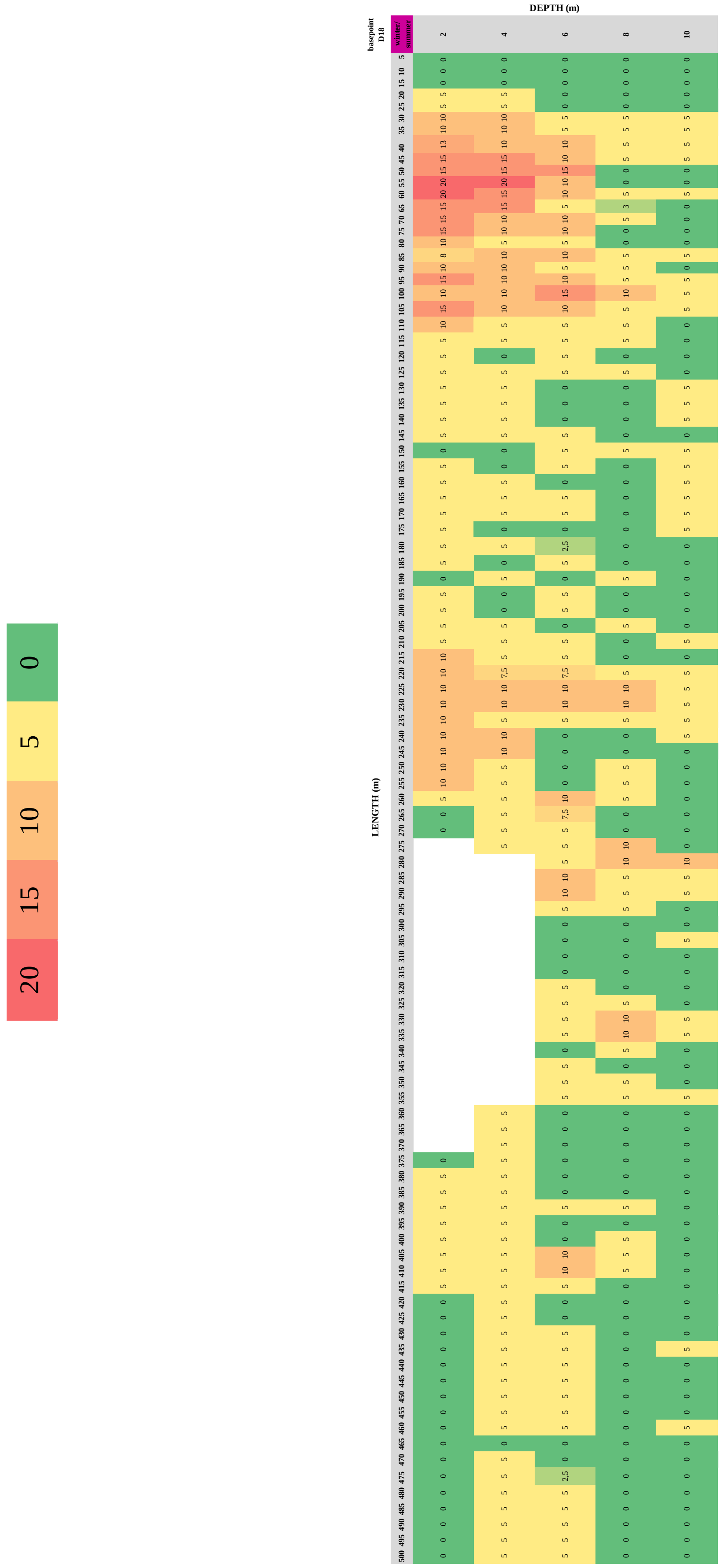

Chart 4.4. – Temperature differential of the summer and the winter season, No. 1a [14]

4.6. LONG-TERM PERIOD ANALYSIS OF HORIZONTAL GROUND HEAT EXCHANGER OPERATION

The analysis carried out in this work was performed using commercial software COMSOL Multiphysics 5.6. Heat transfer can be predicted using the software by solving three conservation equations for continuity, momentum and energy. The numerical modelling of horizontal ground heat exchanger (HGHE) in several variants would provide a realistic condition. The simulation includes long-time operation period of HGHE, of exact shape and the thermal effect of the saturated subsoil and possible underground water flow in shallow region that should also contribute to higher heat exchange rate. Each variant is computed for one year operation, and the time step is one day.

4.6.1. Heat transfer in exchanger

This interface was used to model heat transfer by conduction and convection in pipe of circular shape, in its simplest form like an uninsulated piping system, where the fluid velocity and pressure are known a priori. It provides to define the pipe flow profile and the temperature profiles of each segment, thus the heat transfer is combined with fluid flow analysis already to achieve an accurate estimation of the fluid physical properties related to fluid flow such as a density and a viscosity. All the equations used in this physical process can be found in Chapter 3 – CALCULATION PART.

4.6.1.1. <u>User inputs for the heat transfer in pipe computation</u>

For the pipe heat transfer modelling in COMSOL it is necessary to define these user inputs:

1. Definition of piping system
2. Fluid model selection (Newtonian, Power-law, Bingham)
3. Temperature discretization
4. Identification of the fluid flowing through the piping system
5. Physical properties of the fluid (density, dynamic viscosity, tangential velocity, heat capacity, ratio of specific heats, thermal conductivity)
6. Determination of pipe properties (shape, diameter, flow resistance)
7. Determination of inlet temperature and initial temperature
8. Point selection of outlet temperature
9. Definition of wall heat transfer settings

4.6.2. Heat transfer in subsurface

Porous media models contain empirically determined flow resistance in the model area, which is defined as porosity. Basically, the porous medium model adds a momentum in the momentum control equation. As a result, an assumptions and limitations should be respected in modelling.

The model content only single-phase porous medium for which it was used formulation of surface and physical velocity. Picture 4.7 describes a classification of the transport phenomena in porous media based on the single-and two-phase flow through the pores. Description of transport of species momentum and energy, chemical reactions (endothermic or exothermic) and phase change (solid/liquid, solid/gas and liquid gas) at the differential, local phase-volume level and the application of the volume averaging theories lead to a relatively accurate and yet solvable local description. [24]

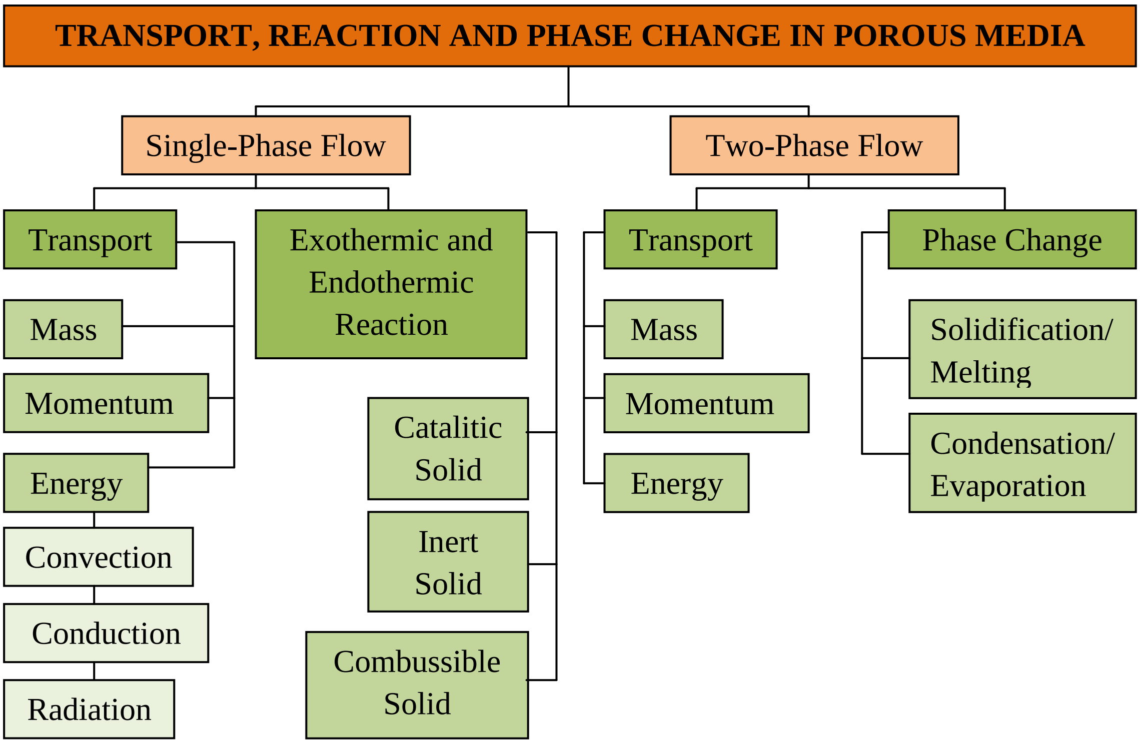

Picture 4.7. – Aspects of treatment of transport, reaction and phase change in porous media [24]

4.6.2.1. <u>User inputs for the porous media computation</u>

For modelling porous media in COMSOL it is necessary to define these users inputs:

1. Selection of porous zone
2. Discretization selection of temperature
3. Identification of the fluid flowing through the porous medium
4. Physical properties of the fluid (density, heat capacity, ratio of specific heats, thermal conductivity)
5. Determination of initial temperature
6. Definition of porosity
7. Definition of heat transfer settings

4.6.3. Model building

The conditions for the choice of collectors are given primarily by the geological situation and the location. It is more a matter of finding a proper construction method, related to the special geological conditions at the site for installation. Based on these considerations, in such a case as a good choice seems to be a closed horizontal system. One of the first consideration factor, which plays a main role in choosing a given system, is known high ground temperature at the certain deep level. The other factors are investment and requirement for a space to erect it. Compared to the vertical loops this system takes a less investment and there is enough space to construct.

The computational domain geometry and parameters follow from the general layout of the ground heat exchanger (GHE) and its construction technology. The reference case consists of the block – ground volume, 20 m width, 22 m long and 10 m depth and of the collector pipe with installation depth 2 m. Axial distance between individual pipes is 1 m. Total length of the loop is 175 m. Structural scheme of GHE is stated bellow – Scheme 4.1. The horizontal loop is connected in series, named meander way that it is shown in the Picture 4.8. This sort of the pipe layout ideally spread extract of heat.

Picture 4.8. – Layout of the pipe

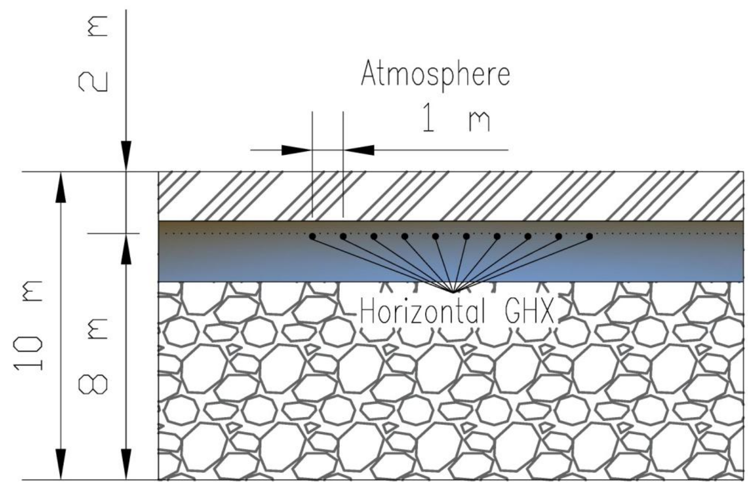

Scheme 4.1. – Structural scheme of GHE

The mesh size of the domain is an essential aspect for numerical simulations, since it is important to avoid boundary effects. In the Picture 4.9., it is possible to see the mesh composed of tetrahedral elements. A computational grid nearby exchanger is denser as better results need to be achieved. The default quality measure is skewness.

Domain element statistics:

- element type: tetrahedron;
- number of elements: 212 720;
- minimum element quality: 0,1824;
- mesh volume 4 400 m^3.

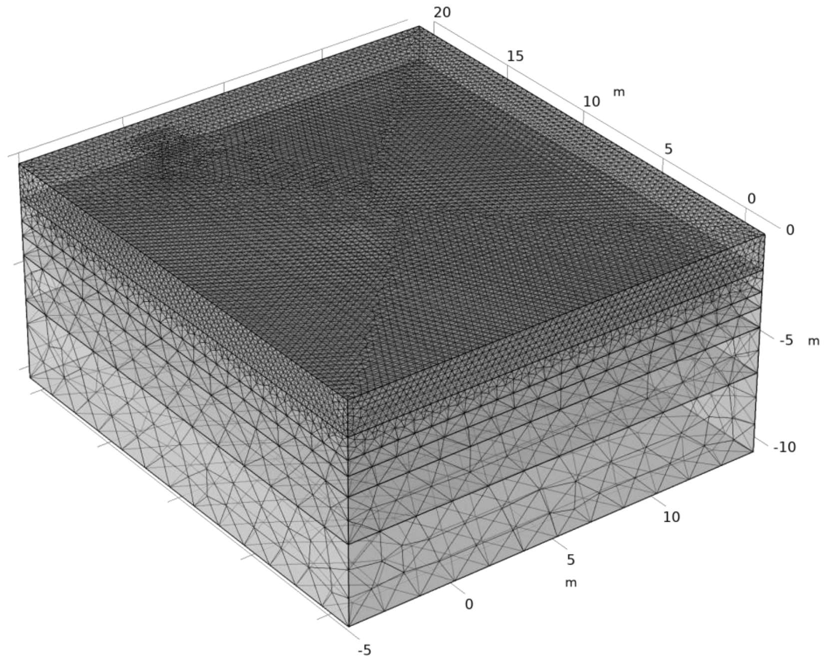

Picture 4.9. – Schematic of the mesh

4.6.4. Material selection

Variety materials are used for a primary circuit of the heat pump earth-water, from metallic to hardened plastic. Decisive factors, for the pipe material selection is heat transfer coefficient and surface roughness.

For HGHE it is possible to use these materials: [25]

- PP – polypropylene;
- PE – polyethylene ;
- HDPE – high density polyethylene;
- galvanized steel;
- titanium;
- copper.

Improvements in heat transfer efficiency can be ensured by choosing material with high thermal conductivity. The higher that value is for a particular material, the more rapidly that heat will be transferred through that material. Copper is one of the materials used for horizontal loop with the highest thermal conductivity.

However, a one question appear, if it is possible to use this type of material when designing horizontal loop in the areas of geothermal activities, thus the one main aspect that merits attention is the correct selection of reliable construction material in such a case. Certain problems may occur regarding the corrosion, pipe scaling and the usage of the materials that are influence the effectiveness and the quality of the service. The knowledge of the ground water characteristics can partly leading to the breakdown of the equipment used for processes due to the corrosion. Previous researches have shown that natural healing water, respectively groundwater is very aggressive towards metallic materials as it contains dissolved carbon dioxide, hydrogen sulphide, orthosilicic acid and sodium of pH 6,85. The possible selection narrows to the plastic pipe.

Based on those considerations, a thermally enhanced polyethylene pipe of dimension 40 x 3 mm was chosen, as the most suitable material for piping which best meets requirements from better heat transfer point of view and the effects of groundwater (Picture 4.10.).

Picture 4.10. – Thermally enhanced polyethylene pipe [32]

Thermal conductivity enhanced PE has the highest thermal conductivity among thermoplastic, 1,2 – 2,2 $W.m^{-1}.K^{-1}$ compared to ordinary PE (0,46 $W.m^{-1}.K^{-1}$) with excellent chemical resistance, resistance to solutions of salts and acids. The recommended long-term service temperature is in the range of – 40 °C up to + 80 °C. Adding graphite is one good option, due to its availability and low cost. Recent technological advances allow the addition of carbon nanoparticles as another efficient method. The challenge is to balance the addition of both coarse and fine particles with the goal of maximizing conductivity, while minimizing the subsequent effects to viscosity and mechanical strength. [28]

4.6.5. Initial and boundary conditions

To ensure proper heat transfer and performance of GHE, it is necessary to define physical properties of each soil layer and pipeline videlicet heat capacity, thermal conductivity, porosity, density and flow rate. The thermal conductivity and the heat capacity change in temperature dependence, that it is stated in Chart 4.5 and Chart 4.6..

Heat capacity is a measure of the ability of the material absorbs thermal energy. This thermophysical property has a weak temperature dependence at high temperatures (above Debye temperature θ_D) however, decreases down to zero as T approaches 0 K. [49]

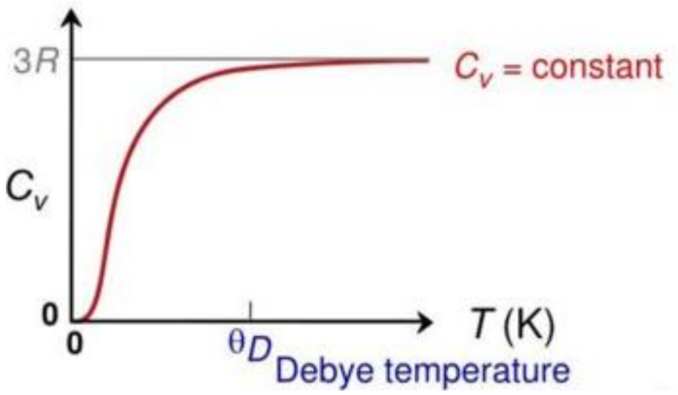

Chart 4.5. – Temperature dependence of heat capacity [49]

Thermal conductivity λ is temperature dependent and is usually determined experimentally by methods based on Fourier´s Law, described by equation 4.1.: [10]

$$\lambda = \frac{q}{-\frac{dT}{dx}} \qquad (4.1.)$$

For saturated liquids and vapours, and gases, of engineering importance, thermal conductivity for most of them decreases with increasing temperature. The exception is water, which exhibits increasing λ up to about 150 °C and decreasing λ thereafter. Water has the highest thermal conductivity of all liquids. [10]

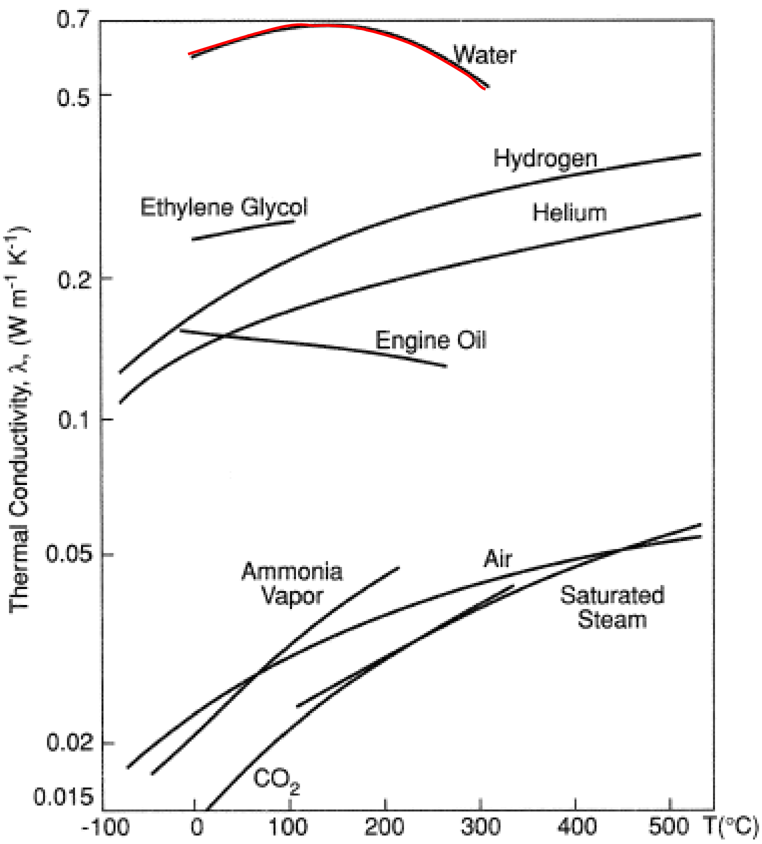

Chart 4.6. – Temperature dependence of various fluids thermal conductivity [10]

In the Tables 4.5. – 4.8.; a main properties of the entire domain are specified.

Table 4.5. – Input values for a soil

SOIL		
Property	Value	Unit
Thermal conductivity	0.7	W/(m.K)
Density	1 800	kg/m^3
Heat capacity at constant pressure	1 480	J/(kg.K)
Ratio of specific heats	1	1
Temperature	50	°C

Table 4.6. – Input values for a saturated soil

SATURATED SOIL		
Property	Value	Unit
Thermal conductivity	1.482	W/(m.K)
Density	1 560	kg/m^3
Heat capacity at constant pressure	1 680	J/(kg.K)
Porosity	0.4	1
Ratio of specific heats	1	1
Temperature	50	°C

Table 4.7. – Input values for a coarse gravels

COARSE GRAVELS 10 – 12 cm		
Property	Value	Unit
Thermal conductivity	0,64	W/(m.K)
Density	1 650	kg/m^3
Heat capacity at constant pressure	755	J/(kg.K)
Ratio of specific heats	1	1
Temperature	50	°C

Table 4.8. – Input values for a pipe

PIPE		
Property	Value	Unit
Thermal conductivity of pipe	1,7	W/(m.K)
Pipe radius	20	mm
Surface roughness	0	mm
Fluid	water	-
Velocity	0,2	m/s
Inlet temperature	10	°C

4.6.6. Analysis and results for constant soil temperature

The first of the possible phenomena can occur in Spa Island is constant 50 °C temperature in the subsoil from 2 m up to 10 m depth, where only top layer is affected by climatic conditions due to unknown temperature at this depth. This consideration is based on several ten-year spa operation and daily pumping of natural healing water of more than 66 °C.

In the Picture 4.11., it is possible to see dynamic behaviour of the subsoil at initial state, thus at time 0, next one after 5 days and 10 days operation. The undisturbed ground temperature is defined as the initial temperature of the entire simulation domain, 50 °C from 2 m depth and surface temperature determined by climatic data. The temperature of the ground is constant and uniform. There is no infiltration and evapotranspiration of precipitation in the modelled area. The modelled area is considered as a homogeneous, isotropic porous medium. By comparing the first one and last result it is evident that only in the first layer changes occur. From the second layer the ground is immutable even after 365 days of ground heat exchanger operation. This fact is subsequently reflected at the outlet temperature from the horizontal loop, that it is shown in the Picture 4.12.. A laminar flow is considered for the simulation. Along the entire exchanger inlet water temperature is 10 °C, it means at initial state. Detailed outputs of this study are stated in ANNEX 8.4.

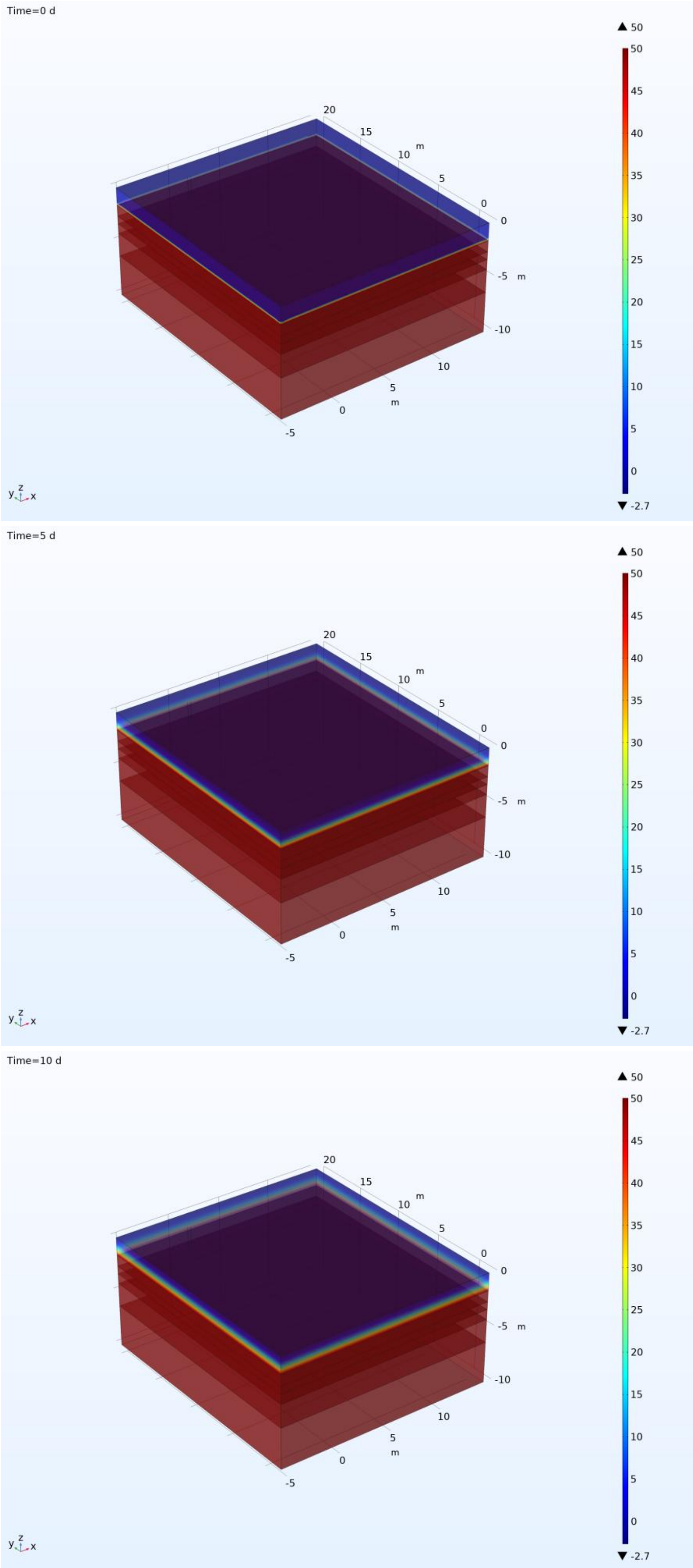

Picture 4.11. – Dynamic behaviour of the subsoil at initial state, 5th day and 10th day of operation

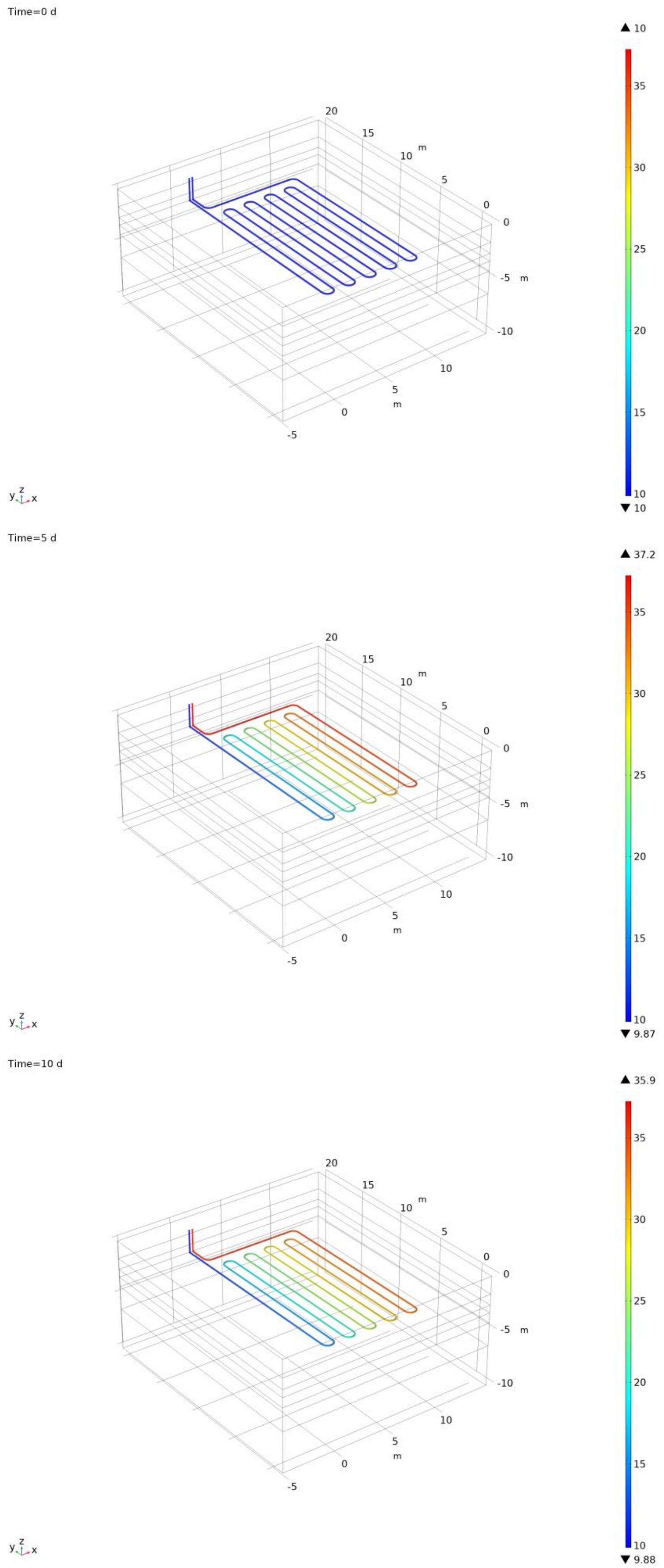

Picture 4.12. – GHE temperature profile for the constant soil temperature

The maximum outlet temperature is reached in 1 day at 44,1 °C, that it is state in Chart 4.7.. However, the temperature starts to decrease after this time period. Thermal equilibrium occurs between ground and fluid in the pipeline. Outlet temperature has stabilized at 35,6 °C within 10 days (Chart 4.8.). It is possible to observe in the Chart 4.7., there are small amplitudes in the beginning and in the end of the pipeline. It is caused by neglecting of thermal insulation.

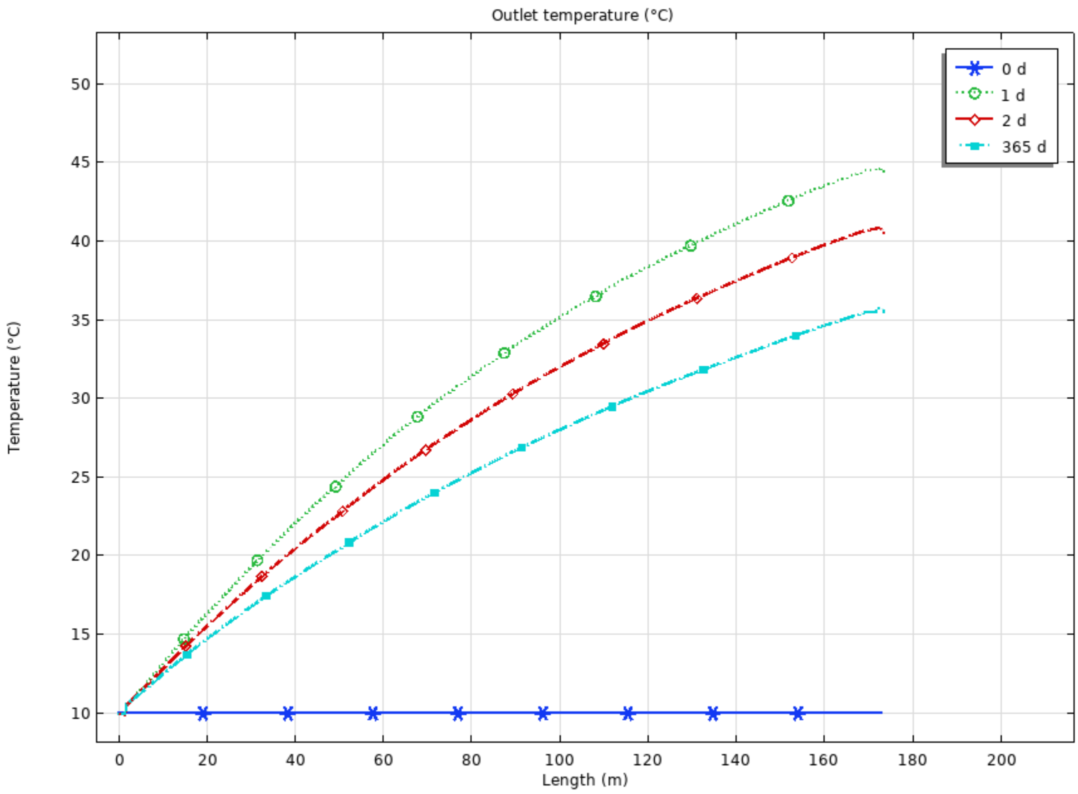

Chart 4.7. – Outlet temperature for constant soil temperature

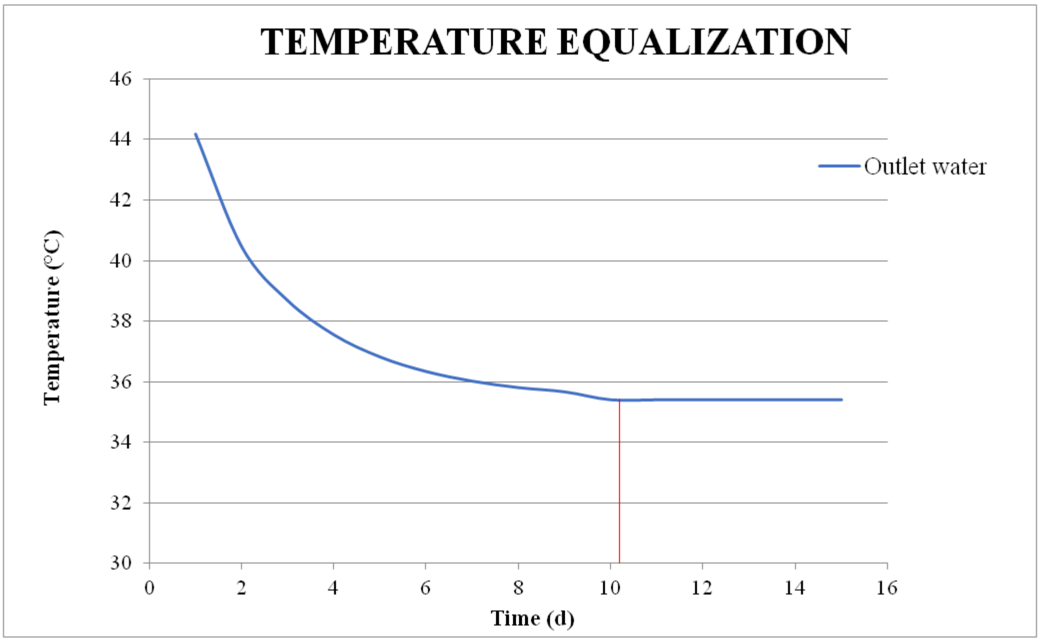

Chart 4.8 – Outlet temperature stabilization

4.6.6.1. Partial conclusion

In this section, the aim of the study was thermal analysis of horizontal ground heat exchanger and saturated subsoil under the constant boundary temperature condition of the ground at Spa Island and determining if a heat pump is required. The analysis was processed numerically by using multiphysics simulation software COMSOL, which work within finite element method (FEM) framework. The soil temperature distribution and the outlet temperatures of HGHE were investigated.

The thermal boundary condition 50 °C, was set up for an entire simulation domain from 2 m depth as a constant and the surface temperature was determined by climatic boundary condition. Infiltration and precipitation evapotranspiration were neglected. Primary circuit of heat pump is placed in second strata of subsoil. As there is not required to use refrigerant, the service water of 10 °C temperature is circulating along the whole horizontal loop. The fluid velocity is 0,2 m/s.

Based on the dynamic thermal model results of subsoil it is apparent that, the ground is almost immutable from the second soil layer even after 365 days of GHE operation. Thermal alterations appear in the first layer and around the pipe only. The temperature changes in the first strata are caused by climatic condition of location of interest. It is evident, if the heat is extracted and transferred then a cold field is created around the pipe system. This fact is subsequently reflected at the outlet temperature from the horizontal loop. As the numerical simulation was computed for one year-round with step one day, the maximum temperature was reached in 1 day at 44,1 °C and after this time period starts to decrease. Between the ground and the loop thermal equilibrium occurs. The temperature has stabilized within 10 days at 35,6 °C and it does not modify to any further extent.

Thanks to this analysis it is concluded that the significant thermal alterations do not interfere due to the operation of horizontal ground heat exchanger under this possible fascinating phenomena that occur at Spa Island. In other words, there is no negative environmental impact in accordance of thermal interfaces in subsurface as well as towards to reduce carbon footprint by exploiting the passive energy without necessity to install a heat pump.

4.6.7. Analysis and results for inconstant soil temperature

Another case study is focused on dynamic behaviour of the HGHE at unstable soil temperature. The initial conditions are determined in the same way as in the previous numerical simulation, thus 50 °C from 2 m depth, surface temperature is defined by monthly climatic data, water flow rate in the pipe is 0,2 m/s and other thermophysical properties remain the same. The only thing has changed is temperature condition.

From a constant temperature state in subsoil, the condition has changed to unstable one, respectively inconstant temperature. The aim of this is study is identifying of potential impact on the environment under such a condition.

Symmetrical cooling over the entire subsurface occurs, however no freezing appear during year-round steady running due to the sufficient soil saturation, whether in the area of GHE or in the whole subsoil. This veritableness is illustrated bellow in the Picture 4.13. From the third image sequence, time 60 d, we can observe cooler temperature field under the loop when the heat is extracted. The minimum temperature nearby GHE after 365 days of operation is 13, 6 °C. As the image sequences are relatively small, a couple of them are listed in ANNEX 8.5.

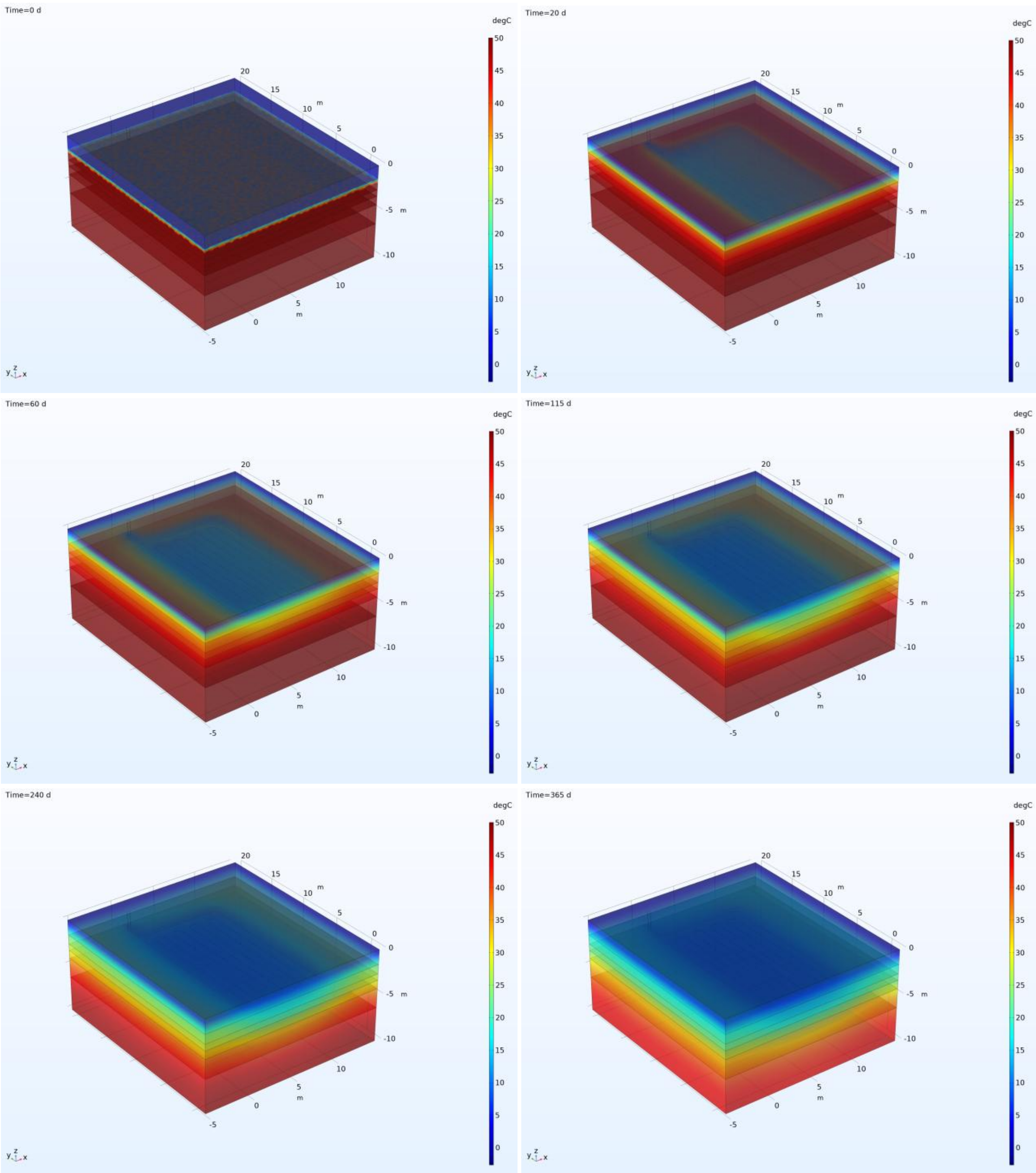

Picture 4.13. – Image sequences of subsurface symmetrical cooling

The temperature profiles of the exchanger are shown in the Picture 4.14., for initial state, for 20^{th}, 60^{th}, 115^{th}, 240^{th} and 365^{th} day and the outlet temperatures are stated in the Chart 4.9.. In the first days of operation temperature changes are minimal compared to the first interface. After 1 day of GHE running, the outlet temperature is 43,1 °C, it means, only 1 °C temperature difference . The outlet temperature from the pipe afterwards 365^{th} day is 11 °C. In such instance, the temperature is not adequate for floor or wall heating, therefore it is necessary to consider a heat pump installation with service water using as a refrigerant is not needed. This will ensure a possible environmental negative impact on groundwater quality and contamination unlikely case of pipe leakages.

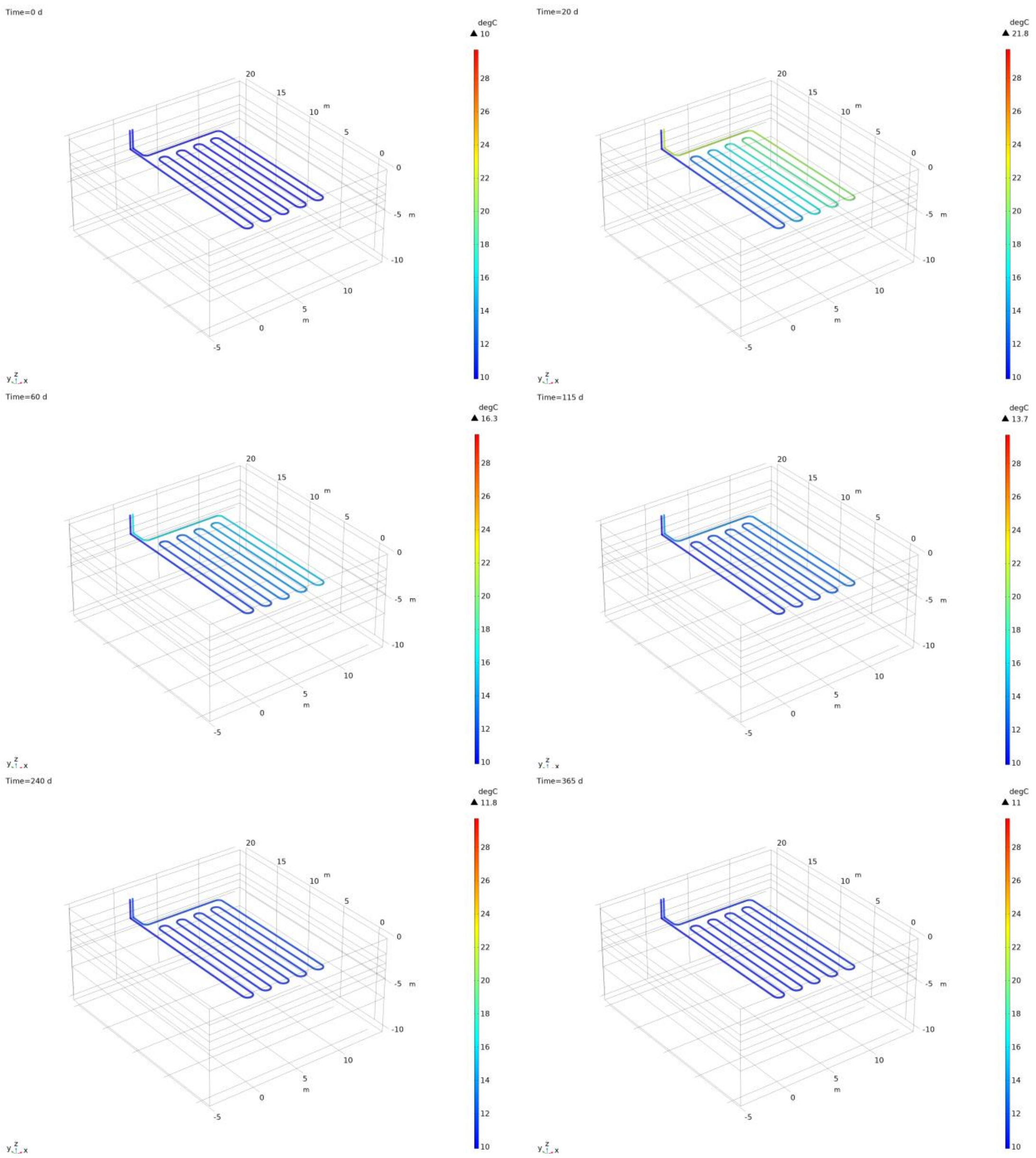

Picture 4.14. – GHE temperature distribution for inconstant soil temperature

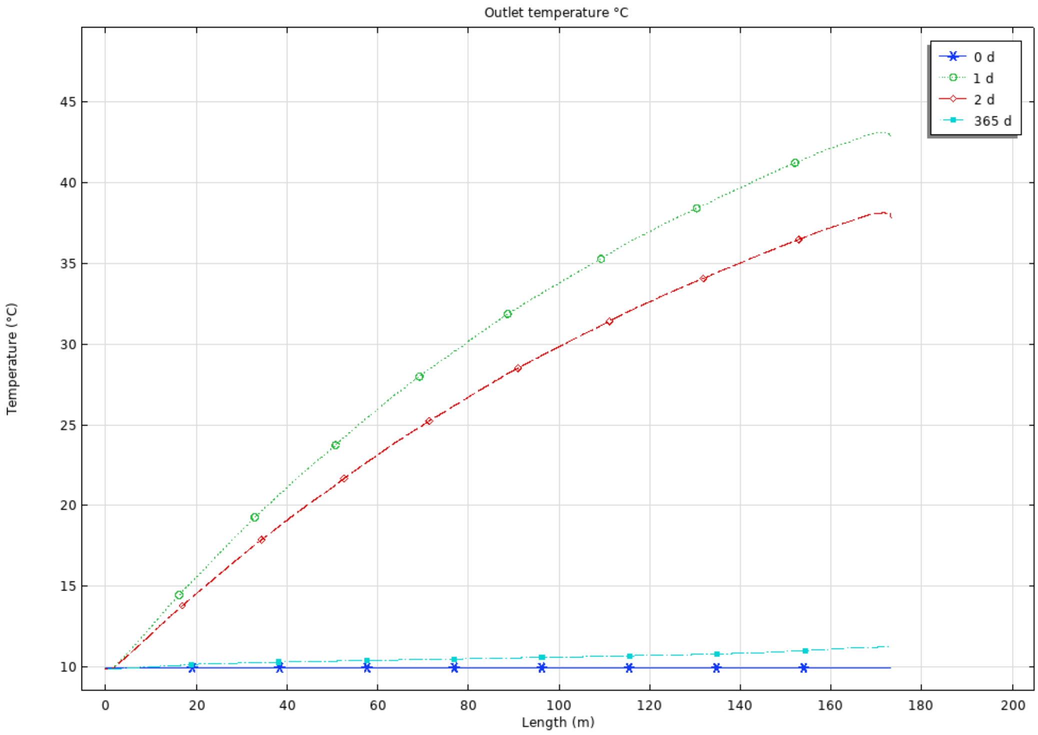

Chart 4.9. – Outlet temperature for inconstant soil temperature

4.6.7.1. Partial conclusion

The second case study was focused on analysis of dynamic process of ground heat exchanger and saturated subsurface under the inconstant temperature boundary condition. The finite element method has been applied to develop a dynamic three-dimensional model for a primary circuit of ground source heat pump using COMSOL software again.

The initial and boundary conditions are determined in the same way likewise in the prevenient numerical simulation. The surface temperature has been set on by interpolation of climatic data for interest location and the ground temperature has been defined as a initial temperature of 50 °C and the velocity of service water circulating inside the pipe system is 0,2 m/s. Only one matter has changed, the temperature condition from constant has changed to inconstant temperature. Such an option must be assumed in this reference study as well.

In this study, the temperature boundary condition transform has a noteworthy effect on the thermal alteration in subsoil during the year-round steady GHE running. There is a rapid symmetrical cooling of the entire subsoil domain, however no freezing appear. This circumstance is caused by the sufficient soil saturation with minimum temperature nearby the area of GHE 13,6 °C afterwards 365 days of operation. It manifests itself similarly at the outlet temperature from pipe after 365th day is 11 °C. In such a representative case, the temperature is not sufficient for floor or wall heating, therefore the heat pump installation has to be considered.

4.6.8. Analysis and results for groundwater flow condition

In this study, the ground heat exchanger is subjected to heat transfer performance with groundwater flow that affects heat exchange efficiency. 3D finite element modelling is used to simulate heat exchange in the HGHE with groundwater flow in the same strata as the HGHE is installed, thus in the second layer. The program combine the saturated soil transient heat transfer equation and Darcy flow equation coupling effect of soil. Meanwhile, the fundamental heat transfer equation for fluid in the pipe and heat transfer for porous medium.

For the computation of this interface the most important boundary conditions are porosity, hydraulic head and hydraulic conductivity. The hydraulic conductivity of the layer is isotropic and the value was determined using a table of various materials which commonly occur in geoenvironmental engineering, namely $5{,}6.10^{-6}$ m/s. Another the key parameter describing a groundwater system is a hydraulic head consists of pressure head and elevation head. Because groundwater velocity is so slow, kinetic energy is typically negligible. As there are not enough measurements of water level, it was not possible to establish exact value. For this reason, the low value was determined (Picture 4.15.). The other initial boundary conditions remain the same as in the previous model. A steady-state Darcy flow under groundwater flow condition was adopted.

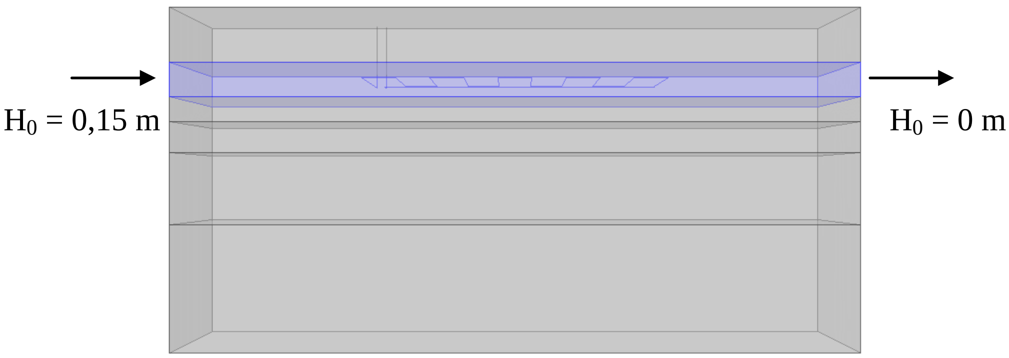

Picture 4.15. – Hydraulic head specification

The Darcy velocity is $4{,}13\ .10^{-4}$ $m.s^{-1}$ in the simulation carried out for this study, that it is illustrated bellow in the Picture 4.16., by streamlines which are instantaneously tangent to the velocity vector of the flow, thus it signifies a direction of natural healing water.

It is clear from Picture 4.17., which even a modest flow rate can have a quite significant effect on thermal regime and the thermal influence of the HGHE is being extended in the direction of flowing water. Temperature contours in horizontal planes indicate that the heat is dissipated along with the water and therefore the temperature field is no longer axially symmetrical in this case.

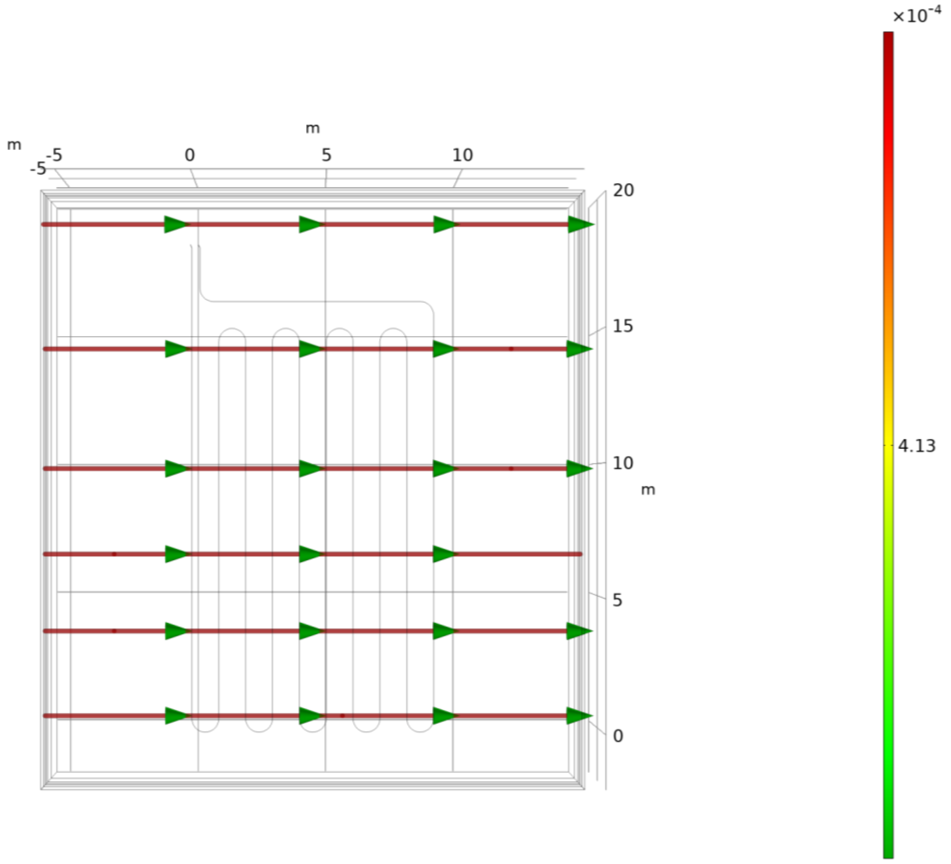

Picture 4.16. – Darcy´s velocity field

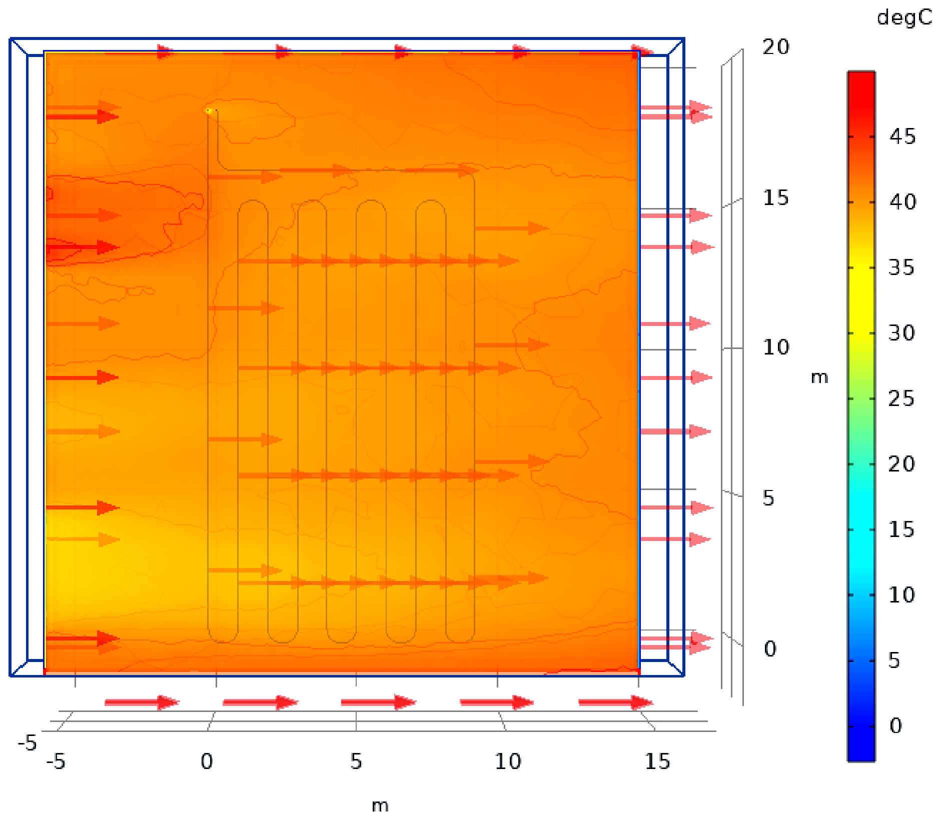

Picture 4.17. – Heat flow profile

As there are three processes of heat transfer: conduction, dispersion and advection, caused by groundwater flow, the temperature distribution along the entire exchanger differ significantly from the previous studies, shown in the Picture 4.18. This causes the temperature on the outlet side to increase. The outlet temperatures of this study are plotted in Chart 4.10. for initial state, 1st, 2nd and 365th day. Along the pipeline there are visible amplitudes which do not occur in previous studies. It is mainly due to the hydraulic conductivity parameter and the porosity. In other words, it is cause by velocity of the groundwater flow. An interesting observation in this case is that the effect of the groundwater flow increases the outlet temperature by an average of 26,7 %, under the same main boundary conditions. Comparison of the outlet temperatures between groundwater flow interface and without groundwater flow interface are stated in the Table 4.9.. Therefore, the results indicate that the influence of groundwater flow should not be neglected.

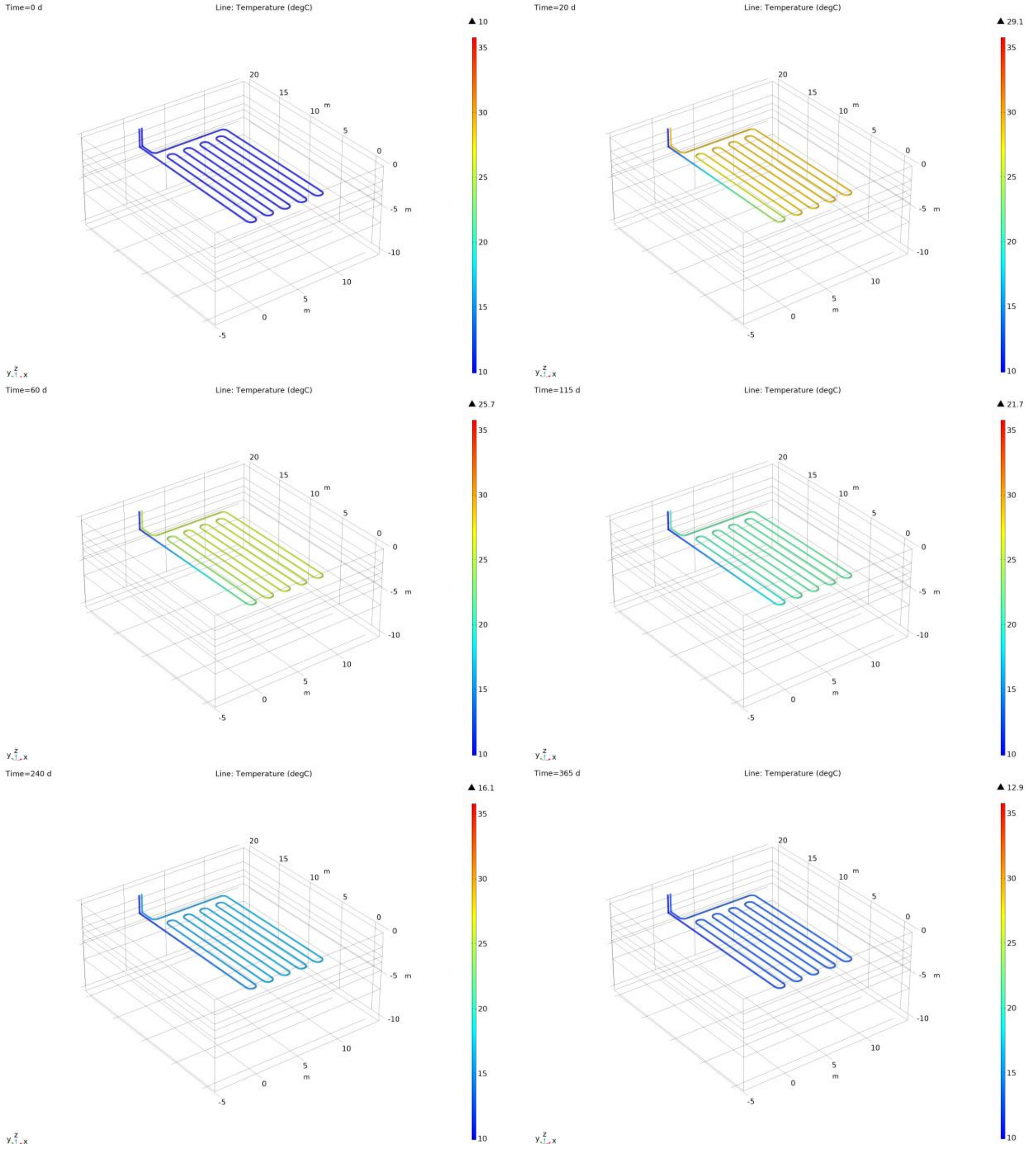

Picture 4.18. - GHE temperature distribution with groundwater flow

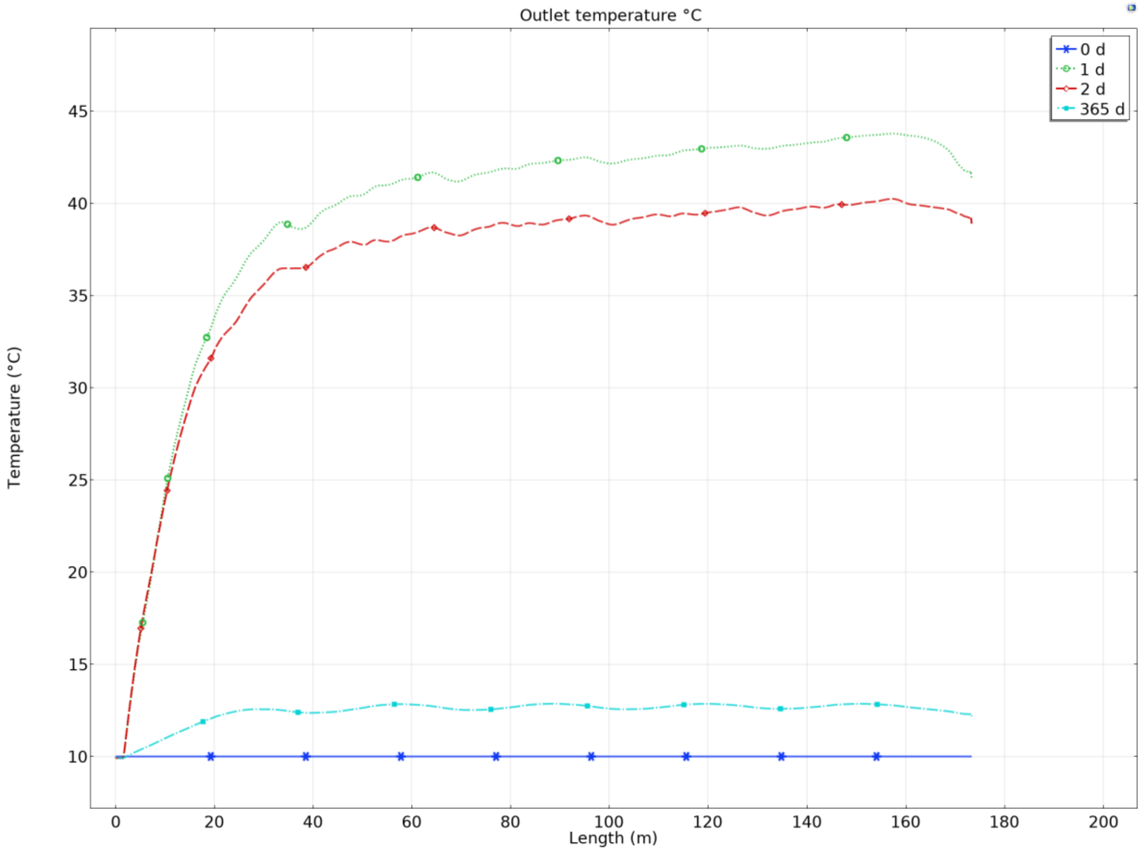

Chart 4.10. – Outlet temperatures from the pipeline under the groundwater flow condition

Table 4.9. – Outlet temperatures comparison

COMPARISON OF OUTLET TEMPERATURES		
TIME (d)	**WITHOUT GROUNDWATER FLOW**	**WITH GROUNDWATER FLOW**
0	10,0 °C	10,0 °C
20	21,8 °C	29,1 °C
60	16,3 °C	25,7 °C
115	13,7 °C	21,7 °C
240	11,8 °C	16,1 °C
365	11,0 °C	12,9 °C

After the carrier fluid has been transported through the pipes, the temperature reached afterwards 365th day of operation is 12,9 °C under groundwater flow condition and 11,0 °C under the resting groundwater condition, which is not enough to use for heating. Therefore in both cases, there is necessary to think about the installation of heat pump which compresses the fluid to generate the desired temperatures (Scheme 4.2.). More detailed outputs of this analysis are listed in ANNEX 8.6., including subsoil temperature distribution.

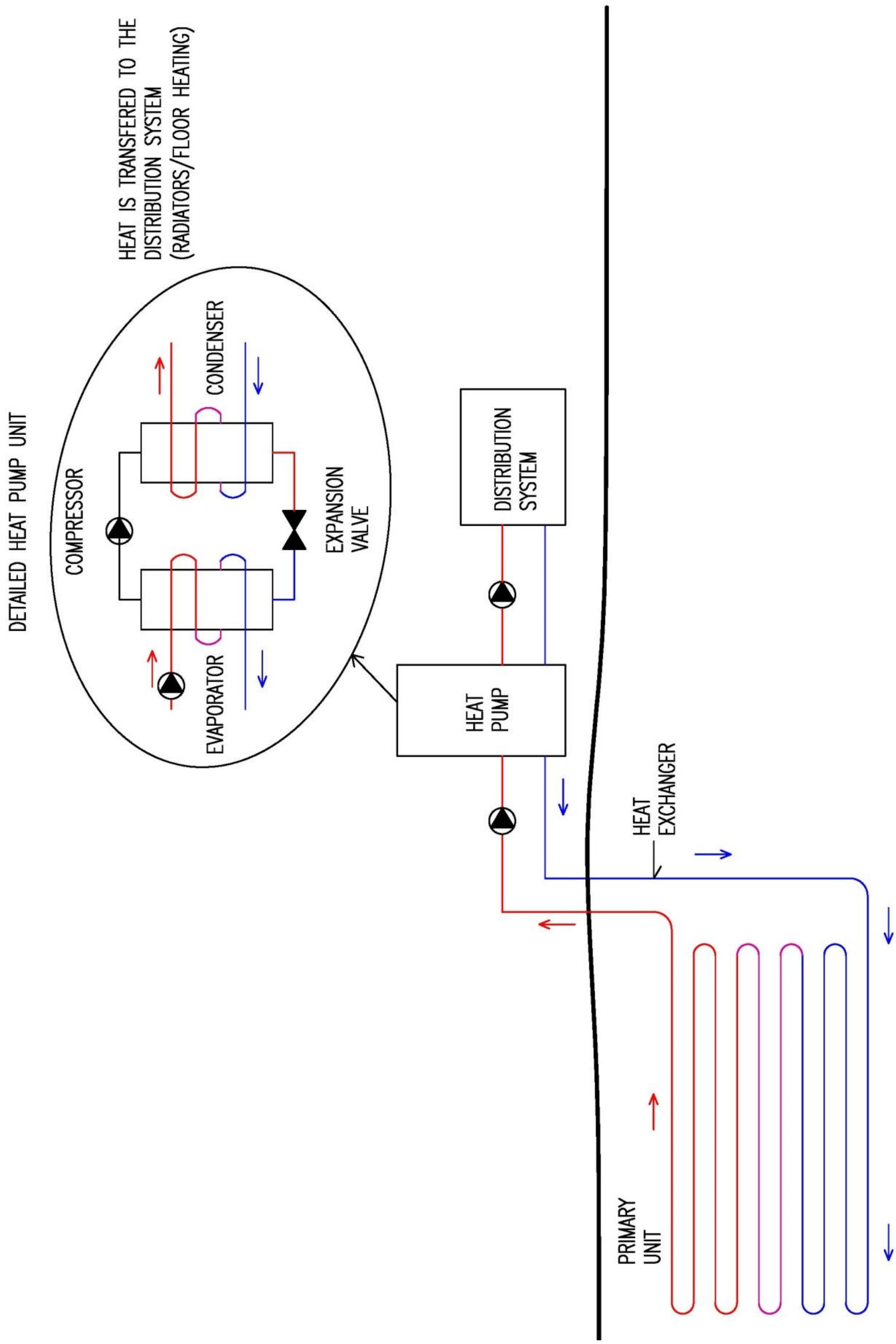

Scheme 4.2. – Connection scheme of ground source heat pump

4.6.8.1. Partial conclusion

Based on previous researches and project documentations of spa, the last analysis was carried out to assessment the horizontal ground heat exchanger operation with possibility of groundwater flow in the same strata and the impact on thermal performance under such a condition. A numerical approach, using the software COMSOL, was utilized to simulate conductive and convective heat transfer between carrying fluid and the surrounding materials as a pipe, soil and groundwater. The software combines heat transfer equations and Darcy flow equation. In this analysis, velocity field, heat flow profile, outlet temperatures and comparison of the outlet temperatures were investigated for 1 year period.

Darcy´s law was used to calculate the circulation velocity under steady state condition. To achieve the velocity of groundwater flow, there are three major parameters that were needed to be identified: hydraulic conductivity, hydraulic head and porosity. The hydraulic conductivity was determined using a table of various materials which commonly occur in geo-environmental engineering, namely $5{,}6.10^{-6}$ m/s for clay-sand soil. As there were not enough measurements of water level, it was not possible to set up exact value of hydraulic head therefore difference between the in and outflow of the flow simulator was determined as low value (15 cm). The porosity remain the same as in the previous studies, thus 0,4 as well as the other thermo-physical properties of soil and pipeline and boundary conditions too. The groundwater flow with specific discharge which corresponds to a Darcy velocity of $4{,}13\ .10^{-4}$ m/s.

As a result of this analysis it is concluded that the modest flow rate have a significant effect on thermal regime and the thermal performance of HGHE, accordingly it contribute to higher exchange rate. Leaving temperatures from the primary circuit of heat pump differ significantly from the previous study. The effect of the groundwater flow increases the outlet temperature by an average of 26,7 %, compared to the resting groundwater. The results signify that the influence of groundwater flow should not be neglected, although the exact values are unknown and determined by engineering tables only. However, the achieved temperature 12,9 °C is still not adequate for heating, for this reason, installation of the heat pump has to be taken in consideration. Such an analysis requires future experimental measurements and evaluations to obtain accurate data of water level, possibly groundwater velocity and soil porosity for a precise numerical simulation.

5. CONCLUSION

Master thesis „Analysis of boundary conditions of ground heat exchangers" was primarily focused on preliminary examination of boundary conditions and key factors influencing the design and heat transfer of ground heat exchangers in geothermal fields at Spa Island in Piešťany. Long-term temperature changes of the ground, related to the operation of the ground heat exchanger were investigated in three possible cases that may occur in area of geothermal fields. These studies were processed by numerical simulation using finite element software – COMSOL Mutiphysics.

One of the main aspects that have been taken into account is related to a site specific condition. This limitation can lead to a go or a no-go for project concept especially due to the negative environmental impact as a contamination of the ground and the groundwater by horizontal ground heat exchanger connecting to the surface, reliable material selection and fluid selection circulating inside the pipe that may affect the chemistry and bacterial composition and growth in the underground unlikely case of pipe leakages and change of the subsurface temperature. As a result, thermal enhanced polyethylene material with the highest thermal conductivity from the plastics range was chosen to achieve the higher heat transfer efficiency as a previous researches has shown an aggressive effect of groundwater towards metallic materials. In case to damage of piping system, the most reasonable choice of fluid flowing inside the pipeline was service water as a refrigerant is not needed due to the sufficient temperature in the subsoil. Considering the fact, that heat transfer efficiency is not influenced by thermo-physical properties of material used for a primary circuit of heat pump only but mainly, it depends on thermal and hydraulic properties of subsoil, especially in case of saturated soil. Thermal conductivity of soil increases with increasing moisture content. For this reason, the subsoil was subjected to an analytical calculation of thermal conductivity established by scientists Johansen and by Côte and Konrad of result value 1,4820 $W.m^{-1}.K^{-1}$. Furthermore, climate and ground temperature circumstances play an important role in the design and application of ground heat exchanger. The assessment of climatic conditions in the interest location were drawn from Slovak Hydrometeorogical Institute which falls on 10 years of measured data for mean monthly air temperature and subsequently interpolated. The temperature condition of subsoil has been already investigated in the previous final thesis and determined for high-potential place of 50 °C annually.

Based on these data, aspects and considerations, three numerical analysis of dynamic process of ground heat exchanger and saturated subsurface were investigated. Each variant was computed for one year GHE operation with the one day time step.

The first numerical analysis was subjected to dynamic process of saturated subsoil under the constant boundary temperature condition during 1 year-round steady running of ground heat exchanger. In this study, the subsoil temperature distribution and the outlet temperatures of HGHE were investigated. For an entire simulation domain, the constant temperature of 50 °C was set on from second layer and the surface temperature was defined by climatic boundary condition. Primary circuit of heat pump is placed in second strata of subsoil. The service water of 10 °C is circulating along the whole horizontal loop by velocity 0,2 $m.s^{-1}$. Thanks to this analysis it was concluded that the minimum outlet temperature after 365^{th} day of operation is 35,6 °C and furthermore there is no negative environmental impact in accordance of thermal interfaces in subsurface as well as towards to reduce carbon footprint by exploiting the passive energy without necessity to install a heat pump.

The second numerical analysis was focused on dynamic process of saturated subsoil under the inconstant boundary temperature condition. Initial and boundary conditions are determined in the same way likewise in the previous study. Only one matter has changed, the temperature condition from constant has changed to inconstant temperature. In this study, the temperature boundary condition transform has a noteworthy effect on the thermal alteration in subsoil during the year-round steady GHE running. There is a rapid symmetrical cooling of the entire subsoil domain, however no freezing appear. This circumstance is caused by the sufficient soil saturation with minimum temperature nearby the area of GHE 13,6 °C afterwards 365 days of operation. It manifests itself similarly at the outlet temperature from pipe after 365^{th} day is 11 °C. In such a representative case, the temperature is not sufficient for floor or wall heating, therefore the heat pump installation has to be considered.

The third analysis was carried out to assessment the horizontal ground heat exchanger operation with possibility of groundwater flow in the same strata and the impact on thermal performance under such a condition. Darcy´s law was used to calculate the circulation velocity under steady state condition. There are three major parameters that were needed to be identified: hydraulic conductivity, hydraulic head and porosity. The hydraulic conductivity was determined using a table which commonly occur in geo-environmental engineering, namely $5,6.10^{-6}$ $m.s^{-1}$. As there were not enough measurements of water level, it was not possible to set up exact value of hydraulic head therefore difference between the in and outflow of the flow simulator was determined as low value (15 cm). The porosity remain the same as in the previous studies, thus 0,4. As a result of this analysis it is concluded that the modest flow rate have a significant effect on thermal regime, accordingly it contribute to higher exchange rate. The effect of the groundwater flow increases the outlet temperature by an average of 26,7 % compared to the resting groundwater. However, the achieved temperature 12,9 °C is still not adequate for heating, for this reason, installation of the heat pump has to be taken in consideration.

An experimental measurements and evaluations to obtain accurate data of water level, possibly groundwater velocity and soil porosity are required in the future for a precise numerical simulation. Nevertheless, thanks to these analyses it has been observe that groundwater flow and sufficient saturation of subsoil should not be neglected in any way as lead to higher heat transfer efficiency.

6. LIST OF SOURCES

[1] 95% Renewable Energy World Possible by 2050 with no Technology Breakthroughs. *CleanTechnica* [online]. 2012 [cit. 2021-01-12]. Dostupné z: https://cleantechnica.com/2012/10/02/95-renewable-energy-world-possible-by-2050-with-no-technology-breakthroughs/

[2] *Acedge* [online]. [cit. 2021-01-12]. Dostupné z: http://www.acedge.com.sg/refrigdiv.html

[3] Air to Water Heat Pumps. *Easy AirConditioning* [online]. [cit. 2021-01-12]. Dostupné z: https://easyairconditioning.com/about/air-to-water-heat-pumps/

[4] ATANGANA, Abdon. *Fractional Operators with Constant and Variable Order with Application to Geo-Hydrology* [online]. 1. Academic Press, 2018, 414 s. [cit. 2021-01-14]. ISBN 978-0-12-809670-3. Dostupné z: https://doi.org/10.1016/C2015-0-05711-2

[5] BECKER, Bryan R. a Brian A. FRICKE. *EFFECTS OF SATURATION AND DRY DENSITY ON SOIL THERMAL CONDUCTIVITY* [online]. 1997 [cit. 2021-01-12]. Dostupné z: doi:10.1007/s11440-017-0563-z

[6] *Bright Hub Engineering* [online]. [cit. 2021-01-14]. Dostupné z: https://www.brighthubengineering.com/hvac/5231-what-is-heat-transfer/

[7] BUDOVEC, Michal. *Přenos tepla radiací* [online]. 2016 [cit. 2021-01-12]. Dostupné z: https://www.vutbr.cz/studenti/zav-prace/detail/94052. Bakalářska práce. VUT, Fakulta elektrotechniky a komunikačních technologií.

[8] CÔTÉ, Jean a Jean-Marie KONRAD. *A generalized thermal conductivity model for soils and construction materials*. Canadian Geotechnical Journal, 2011, **42**(2). ISSN 443-458. Dostupné z: doi:10.1139/t04-106

[9] *Danubius hotels* [online]. [cit. 2021-01-12]. Dostupné z: https://www.danubiushotels.com/sk/kupelne-a-wellness/kupelne-mesta/kupelne-hotely-na-slovensku

[10] DAVIES, Thomas W. *THERMAL CONDUCTIVITY VALUES* [online]. 2011 [cit. 2021-01-12]. Dostupné z: doi:10.1615/AtoZ.t.thermal_conductivity_values

[11] DONG, Yi a John S. MCCARTNEY. *Critical Review of Thermal Conductivity Models for Unsaturated Soils* [online]. Switzerland: Springer International, 2015 [cit. 2021-01-12]. Dostupné z: doi:10.1007/s10706-015-9843-2

[12] *Ec europa* [online]. [cit. 2021-01-14]. Dostupné z: https://ec.europa.eu/energy/en/topics/energy-strategy-and-energy-union

[13] FENDEK, Marián, Ondrej FRANKO a Anton REMŠÍK. *Atlas geotermálnej energie Slovenska* [online]. 1. Štátny geologický ústav Dionýza Štúra v Bratislave: Michal Vaško, 2010 [cit. 2021-01-12]. ISBN 80-85314-38-X. Dostupné z: https://apl.geology.sk/mapportal/img/pdf/atlasy/atlas_ge_sj_text.pdf

[14] FLOREKOVÁ, Skarleta. *Boundary conditions for the operation of thermal energy distribution*. Brno, 2018. Bakalářska práce. VUT, Fakulta stavební. Vedoucí práce prof. Ing. Jiří Hirš, CSc.

[15] *Geologické Práce*. Bratislava: Štátny geologický ústav Dionýza Štúra, 2012. ISSN 0433-4795.

[16] *Geotherm* [online]. [cit. 2021-01-12]. Dostupné z: https://www.geotherm.sk/plosne-kolektory/

[17] GHUMAN, B.S. a R. LAL. *Thermal conductivity, thermal diffusivity*. Soil Sience, 1985. Dostupné také z: https://journals.lww.com/

[18] GORENJE. *HEAT PUMPS: Heating Systems*. Velenje, 2013 [cit. 2021-01-12].

[19] Ground Source Energy. *Icax - INTERNATIONAL HEAT TRANSFER* [online]. [cit. 2021-01-12]. Dostupné z: https://www.icax.co.uk/Ground_Source_Energy.html

[20] HALLDÓRSDÓTTIR, Sæunn. *Geothermal reservoir management and sustainable use* [online]. Reykjavík, 2018 [cit. 2021-01-12]. Dostupné z: https://www.slideshare.net/IcelandGeothermal/c3-geothermal-reservoir-management-and-sustainable-use

[21] *Heat Transfer Module User's Guide* [online]. COMSOL, 2018, , 702 [cit. 2021-01-12]. Dostupné z: https://doc.comsol.com/5.4/doc/com.comsol.help.heat/HeatTransferModuleUsersGuide.pdf

[22] *Industrial heat pumps* [online]. [cit. 2021-01-12]. Dostupné z: http://industrialheatpumps./en/how_it_works/cop_heat_pump/

[23] JIROUŠ, Filip. *Renewable energy policy database and support – RES-LEGAL EUROPE, National profile: Slovakia*. Berlin, 2013

[24] KAVIANY, Massoud. *Principles of Heat Transfer in Porous Media*. New York, NY: Springer, 1995. ISBN 978-1-4612-4254-3. Dostupné z: doi:https://doi.org/10.1007/978-1-4612-4254-3_1

[25] KOŠIČANOVÁ, Danica a Andrea FEDÁKOVÁ. Zemné výmenníky tepla. *TechCON*. Bratislava, 2009, **5**(3), 36. ISSN 1337-3013.

[26] LEONARD, Ashley a Will CRAIG. *Mechanical Engineering: An Integrated Approach*. United Kingdom: ED-Tech Press, 2019. ISBN 978-1-83947-243-5.

[27] *Mapy* [online]. [cit. 2021-01-12]. Dostupné z: https://sk.mapy.cz/zakladni?x=16.6333010&y=49.2000010&z=11

[28] MENDRINOS, Dimitrios, Constantine KARYTSAS a Spyridon KATSANTONIS. *Pipe materials for borehole heat exchangers* [online]. Strasbourg, 2016 [cit. 2021-01-12]. Dostupné z: https://www.researchgate.net/publication/328232447_Pipe_materials_for_borehole_heat_exchangers

[29] *Modeling, Simulation and Energy Performance of VFD and ON/OFF Cycle HVAC Systems* [online]. 2016 [cit. 2021-01-12]. Dostupné z: https://www.researchgate.net/publication/323540295_Modeling_Simulation_and_Energy_Performance_of_VFD_and_ONOFF_Cycle_HVAC_Systems. Master Thesis. King Fahd University of Petroleum and Minerals.

[30] MYSLIL, Vlastimil. *Geotermální energie: zdroje, využití, technologie*. Liberec: Geoterm CZ, 2011. ISBN 978-80-260-2349-4.

[31] *NIBE* [online]. [cit. 2021-01-12]. Dostupné z: https://www.nibe.sk/technologia/hlbinny-vrt

[32] *NIBE* [online]. [cit. 2021-01-12]. Dostupné z: https://www.nibe.cz/images/download/Technicky_list_PE100RC_POWER.pdf

[33] *Piešťany-výpočet množstiev minerálnych vôd:* Záverečná správa-hydrogeologický prieskum. Žilina, 2011

[34] *Pipe Flow Module User's Guide* [online]. COMSOL, 2018, , 122 [cit. 2021-01-12]. Dostupné z: https://doc.comsol.com/5.4/doc/com.comsol.help.pipe/PipeFlowModuleUsersGuide.pdf

[35] Počasie a klíma na Slovensku. *Slovakia Site* [online]. [cit. 2021-01-12]. Dostupné z: http://www.slovakiasite.com/weather-and-climate.php

[36] *Prospekt High-Tech Waermepumpen.* 2012 [online] [cit. 2021-01-12]. Dostupné z: https://pdf.archiexpo.de/pdf/ochsner/prospekt-high-tech-waermepumpen/62592-228765.html

[37] *Renewables First* [online]. [cit. 2021-01-12]. Dostupné z: https://www.renewablesfirst.co.uk/water-source-heat-pumps/water-source-heat-pump-benefits/

[38] ROGACHEV, M. S., Yu. I. SHTERN, M. Yu. SHTERN a R. E. MIRONOV. *A heat transfer model of a horizontal ground heat exchanger*. American Institute of Physics, 2016, , 11. Dostupné z: doi:10.1063/1.4945970

[39] *Rozbor vody zo Štátnych kúpeľov Piešťany - hlavný prameň „Trajan"*: Záverečná správa. 1948.

[40] SIEGENTHALER P.E., John. *Water To Water Heat Pumps*. 2000.

[41] *Slide Share* [online]. [cit. 2021-01-12]. Dostupné z: https://www.slideshare.net/gauravhtandon1/ground-water-unitv

[42] *Solar Renewable Installations Ltd* [online]. [cit. 2021-01-12]. Dostupné z: https://solarandrenewable.co.uk/?portfolio=ground-source-heat-pumps

[43] *SWEP* [online]. [cit. 2021-01-12]. Dostupné z: https://www.swep.net/

[44] *Think GeoEnergy* [online]. [cit. 2021-01-12]. Dostupné z: https://www.thinkgeoenergy.com/slovakia-seeing-development-of-first-geothermal-power-plant/

[45] *Topení-chlazení* [online]. [cit. 2021-01-12]. Dostupné z: http://www.topeni-chlazeni.cz/tepelna-cerpadla-zeme-voda/

[46] *Travelettes* [online]. [cit. 2021-01-12]. Dostupné z: http://www.travelettes.net

[47] *Vyhodnotenie sond systému A na Kúpeľnom ostrove Piešťany*: Záverečná správa. 1956

[48] WANG, Jinxin, Ying ZHAO a Hailong HE. A modified normalized model for predicting effective soil thermalconductivity. *Acta Geotechnica* [online]. Springer, 2017 [cit. 2021-01-12]. Dostupné z: doi:10.1007/s11440-017-0563-z

[49] ZHIGILEI, Leonid. *Introduction to Materials Science* [online]. In: . 2010 [cit. 2021-01-12]. Dostupné z: http://people.virginia.edu/~lz2n/mse209/Chapter19c.pdf

[50] ŽERAVÍK, Antonín. *Stavíme tepelné čerpadlo*. 1. Kroměříž: Antonín Žeravík, 2003, s. 312. ISBN 80-239-0275-X.

6.1. LIST OF PICTURES

6.2. LIST OF TABLES

6.3. LIST OF CHARTS

6.4. LIST OF SCHEMES

7. LIST OF ABBREVIATIONS AND SYMBOLS

λ (S)	thermal conductivity at saturation S	($W.m^{-1}.K^{-1}$)
K_e	normalized thermal conductivity	($W.m^{-1}.K^{-1}$)
λ_{sat}	thermal conductivity of saturated soil	($W.m^{-1}.K^{-1}$)
λ_{dry}	thermal conductivity of dry soil	($W.m^{-1}.K^{-1}$)
λ_w	thermal conductivity of water	($W.m^{-1}.K^{-1}$)
ϕ	porosity	(%)
λ_s	effective thermal conductivity of soil solids	($W.m^{-1}.K^{-1}$)
q	quartz content of the total solids	(%)
λ_q	thermal conductivity of quartz	($W.m^{-1}.K^{-1}$)
λ_0	fraction of other minerals	($W.m^{-1}.K^{-1}$)
ρ_b	dry bulk density	($kg.m^{-3}$)
ρ_s	average density of the soil solids	($kg.m^{-3}$)
κ	dimensionless empirical fitting parameter	(-)
ρ	fluid density	($kg.m^{-3}$)
C_p	fluid heat capacity at constant pressure	($J.kg^{-1}.K^{-1}$)
$(\rho C_p)_{eff}$	effective volumetric heat capacity at constant pressure	($J.m^{-3}.K^{-1}$)
k_{eff}	effective thermal conductivity	($W.m^{-1}.K^{-1}$)
q	conductive heat flux	($W.m^{-2}$)
u	velocity field	($m.s^{-1}$)
Q	heat source	($W.m^{-3}$)
ΔH	difference in hydraulic head between two lateral points	(m)
ΔL	distance between two lateral points	(m)
Q_{wall}	external heat exchange through the pipe wall	($W.m^{-1}$)

T	temperature	(K)
f_D	Darcy friction factor	(-)
d_h	hydraulic diameter	(m)
h	heat transfer coefficient	$(W.m^{-2}.K^{-1})$
Z	wall perimeter	(m)
ΔT	temperature differences across the wall	(K)
r_n	outer radius of wall *n*	(m)
Z_n	outer perimeter of wall *n*	(m)
h_{int}	heat transfer coefficient on the inside of the pipe	$(W.m^{-2}.K^{-1})$
h_{ext}	heat transfer coefficient on the outside of the pipe	$(W.m^{-2}.K^{-1})$
k_n	thermal conductivity of wall *n*	$(W.m^{-1}.K^{-1})$
Re	Reynolds number	(-)
c_A	A contribution	(-)
c_B	B contribution	(-)
e	surface roughness	(m)
μ	fluid dynamic viscosity	$(kg.m^{-1}.s^{-1})$

EU	European Union
NHW	Natural healing water
3D	Three dimensional
UGT	Undisturbed ground temperature
GHE	Ground heat exchanger
HGHE	Horizontal ground heat exchanger
GSHP	Ground source heat pump
COP	Coefficient of performance
SPF	Seasonal performance factor

8. LIST OF ANNEXES

8.1. MAP OF OBSERVATION DRILLS
8.2. TABLE OF EVALUATED DRILLS
8.3. HEAT MAP
8.4. DETAILED OUTPUTS OF NUMERICAL ANALYSIS FOR CONSTANT SOIL TEMPERATURE
8.5. DETAILED OUTPUTS OF NUMERICAL ANALYSIS FOR INCONSTANT SOIL TEMPERATURE
8.6. DETAILED OUTPUTS OF NUMERICAL ANALYSIS FOR GROUNDWATER FLOW CONDITION